Published September 11, 2006

Function of a STIM1 Homologue in *C. elegans*: Evidence that Store-operated Ca^{2+} Entry Is Not Essential for Oscillatory Ca^{2+} Signaling and ER Ca^{2+} Homeostasis

Xiaohui Yan,[1] Juan Xing,[1] Catherine Lorin-Nebel,[1] Ana Y. Estevez,[1] Keith Nehrke,[2] Todd Lamitina,[1] and Kevin Strange[1]

[1]Department of Anesthesiology, Department of Molecular Physiology and Biophysics, and Department of Pharmacology, Vanderbilt University Medical Center, Nashville, TN 37232

[2]Department of Medicine, Division of Nephrology, University of Rochester Medical Center, Rochester, NY 14642

1,4,5-trisphosphate (IP_3)-dependent Ca^{2+} signaling regulates gonad function, fertility, and rhythmic posterior body wall muscle contraction (pBoc) required for defecation in *Caenorhabditis elegans*. Store-operated Ca^{2+} entry (SOCE) is activated during endoplasmic reticulum (ER) Ca^{2+} store depletion and is believed to be an essential and ubiquitous component of Ca^{2+} signaling pathways. SOCE is thought to function to refill Ca^{2+} stores and modulate Ca^{2+} signals. Recently, stromal interaction molecule 1 (STIM1) was identified as a putative ER Ca^{2+} sensor that regulates SOCE. We cloned a full-length *C. elegans stim-1* cDNA that encodes a 530–amino acid protein with ~21% sequence identity to human STIM1. Green fluorescent protein (GFP)–tagged STIM-1 is expressed in the intestine, gonad sheath cells, and spermatheca. Knockdown of *stim-1* expression by RNA interference (RNAi) causes sterility due to loss of sheath cell and spermatheca contractile activity required for ovulation. Transgenic worms expressing a STIM-1 EF-hand mutant that constitutively activates SOCE in *Drosophila* and mammalian cells are sterile and exhibit severe pBoc arrhythmia. *stim-1* RNAi dramatically reduces STIM-1::GFP expression, suppresses the EF-hand mutation–induced pBoc arrhythmia, and inhibits intestinal store-operated Ca^{2+} (SOC) channels. However, *stim-1* RNAi surprisingly has no effect on pBoc rhythm, which is controlled by intestinal oscillatory Ca^{2+} signaling, in wild type and IP_3 signaling mutant worms, and has no effect on intestinal Ca^{2+} oscillations and waves. Depletion of intestinal Ca^{2+} stores by RNAi knockdown of the ER Ca^{2+} pump triggers the ER unfolded protein response (UPR). In contrast, *stim-1* RNAi fails to induce the UPR. Our studies provide the first detailed characterization of STIM-1 function in an intact animal and suggest that SOCE is not essential for certain oscillatory Ca^{2+} signaling processes and for maintenance of store Ca^{2+} levels in *C. elegans*. These findings raise interesting and important questions regarding the function of SOCE and SOC channels under normal and pathophysiological conditions.

INTRODUCTION

Changes in cytoplasmic Ca^{2+} levels regulate a diverse array of physiological processes and function as an essential signaling mechanism in virtually all cells (Berridge et al., 2003). Cytoplasmic Ca^{2+} levels are altered by Ca^{2+} flux across the plasma membrane and by release of Ca^{2+} from intracellular stores. The ER is a major source of intracellular Ca^{2+} release, which is mediated by 1,4,5-trisphosphate (IP_3) receptor (IP_3R) Ca^{2+} channels (Berridge et al., 2003). Early studies on parotid acinar cells demonstrated that activation of intracellular Ca^{2+} release was associated with increased plasma membrane Ca^{2+} entry (for review see Parekh and Penner, 1997). Putney (1986) postulated that the Ca^{2+} content of the ER stores directly regulated Ca^{2+} influx across the plasma membrane and that Ca^{2+} entry was activated by store depletion. This process was initially termed capacitive Ca^{2+} entry, but is now known as store-operated Ca^{2+} entry (SOCE). SOCE is thought to be essential for refilling ER Ca^{2+} stores and for modulating the time course and amplitude of cytoplasmic Ca^{2+} signals (Parekh and Penner, 1997; Venkatachalam et al., 2002; Parekh and Putney, 2005).

Hoth and Penner (1992) identified the first store-operated Ca^{2+} (SOC) current in 1992 by patch clamp electrophysiology. This current, termed Ca^{2+} release–activated Ca^{2+} current or I_{CRAC}, has been the most extensively characterized SOCE pathway (Parekh and Penner, 1997; Parekh and Putney, 2005). Despite intense

Correspondence to Kevin Strange: kevin.strange@vanderbilt.edu

A.Y. Estevez's present address is Biology Department, St. Lawrence University, Canton, NY 13617.

T. Lamitina's present address is Department of Physiology, University of Pennsylvania, Philadelphia, PA 19104.

Abbreviations used in this paper: CV, coefficient of variance; DIC, differential interference contrast; FRET, fluorescence resonance energy transfer; I_{CRAC}, Ca^{2+} release–activated Ca^{2+} current; IP_3, 1,4,5-trisphosphate; IP_3R, IP_3 receptor; SCID, severe combined immunodeficiency; SERCA, sarcoplasmic/ER Ca^{2+} ATPase; SOCE, store-operated Ca^{2+} entry; STIM1, stromal interaction molecule 1; UPR, unfolded protein response.

Published September 11, 2006

study, the mechanism by which store depletion activates SOCE has remained unclear until recently. Using an RNAi screen of SOCE in *Drosophila* S2 cells, Roos et al. (2005) identified stromal interaction molecule 1 (STIM1) as an essential component of CRAC activation.

Human STIM1 was identified originally as a potential tumor suppressor gene (Parker et al., 1996; Sabbioni et al., 1997). Two STIM homologues, STIM1 and STIM2, are present in the human genome (Williams et al., 2001). siRNA knockdown of STIM2 has no effect on SOCE in HEK293 cells (Roos et al., 2005) but inhibits HeLa cell SOCE (Liou et al., 2005). Recent studies suggest that STIM2 interacts with STIM1 and may function normally to inhibit SOC channels (Soboloff et al., 2006a,b).

STIM1 and STIM2 each have a predicted single membrane-spanning domain. In the absence of store depletion, STIM1 colocalizes with ER markers (Liou et al., 2005; Zhang et al., 2005). An EF-hand Ca^{2+} binding domain is present on the N terminus of STIM1 and is localized to the ER lumen. Depletion of ER Ca^{2+} stores or disruption of Ca^{2+} binding by mutation of the EF-hand domain induces translocation of STIM1 toward the plasma membrane (Liou et al., 2005; Zhang et al., 2005) with subsequent activation of SOCE (Liou et al., 2005; Zhang et al., 2005) and I_{CRAC} (Spassova et al., 2006).

The nematode *C. elegans* provides a number of experimental advantages for defining the genes and integrated genetic pathways involved in biological processes such as Ca^{2+} signaling (Barr, 2003; Strange, 2003). The worm has a short life cycle, is genetically tractable, and has a fully sequenced and well-annotated genome. It is also relatively easy and economical to manipulate and hence characterize gene function in this organism using transgenic and RNAi methods.

Both the gonad and intestine of *C. elegans* have proven to be useful models for characterizing IP_3-dependent Ca^{2+} signaling pathways using genetic, molecular, and physiological approaches (Clandinin et al., 1998; Dal Santo et al., 1999; Bui and Sternberg, 2002; Estevez et al., 2003; Kariya et al., 2004; Yin et al., 2004; Espelt et al., 2005; Estevez and Strange, 2005; Teramoto and Iwasaki, 2006). We have shown previously that intestinal epithelial cells express SOC channels (Estevez et al., 2003) and have postulated that SOCE plays an important role in gonad function (Rutledge et al., 2001; Yin et al., 2004). The focus of the current study was to characterize the function of STIM homologues in IP_3 and oscillatory Ca^{2+} signaling pathways in *C. elegans*. A single gene, *stim-1*, encoding a predicted STIM1 homologue is present in the worm genome. We demonstrate here that *stim-1* is essential for the normal IP_3- and Ca^{2+}-dependent contractile activity of gonad sheath cells and the spermatheca. *stim-1* RNAi dramatically reduces STIM-1 expression and inhibits SOC channel activity in intestinal epithelial cells but has no effect on intestine oscillatory Ca^{2+} signaling and associated behavioral rhythms or on the intestinal ER unfolded protein response. Our studies provide the first detailed characterization of STIM-1 function in an intact animal and are the first to link this protein to specific whole animal physiological processes. In addition, our results indicate that SOCE is not required for all oscillatory Ca^{2+} signaling processes and raise interesting and important questions regarding the function of SOC channels under normal and pathophysiological conditions.

MATERIALS AND METHODS

C. elegans Strains

Nematodes were cultured using standard methods (Brenner, 1974). Wild-type worms were the Bristol N2 strain. The following alleles were used: *itr-1*(*sa73, sy290, sy327*), *ipp-5*(*sy605*), *lfe-2*(*sy326*), *rrf-1*(*pk1417*), *elt-2::gfp*(*wIs84*), *rde-1*(*ne219*), and *hsp-4::gfp*(*zcIs4*). *itr-1*(*sa73*) is a temperature-sensitive allele. Worms harboring this mutation were grown at the permissive temperature of 16°C. For RNAi experiments, eggs from *itr-1*(*sa73*) worms were placed on RNAi feeding plates and grown at 25°C. All other strains were grown at 16–25°C. Unless stated otherwise, all experimental results presented were from studies conducted on young adult hermaphrodites.

Analysis of Sheath Cell Contraction and Ovulation

Synchronized L1 larvae were grown for 32–36 h at 25°C and then anesthetized in M9 solution containing 0.1% tricaine and 0.01% tetramisole for 20–40 min. Anesthesized worms were mounted onto 2% agarose pads (McCarter et al., 1999) and were imaged at room temperature (22–23°C) by differential interference contrast (DIC) microscopy using a Nikon Eclipse TE2000 inverted microscope and a Superfluor 40X/1.3 N.A. oil immersion objective lens. Images were recorded at 30 frames/s on videotape using a DAGE-MTI CCD100 camera and analyzed offline. Sheath contractions were counted in 1-min intervals. The intensity or "force" of individual contractions was estimated by measuring lateral displacement of the sheath as described previously (Miller et al., 2001).

Measurement of Brood Size

Brood size was quantified at 25°C by transferring single L4 larvae to new growth plates daily for 4 d. The number of progeny on each plate was counted 24–36 h after eggs hatched.

Characterization of pBoc Cycle

Posterior body wall muscle contraction (pBoc) was monitored at room temperature (21–22°C) in young adult worms. A minimum of 10 pBoc cycles was measured in each animal. Worms were imaged using a Carl Zeiss MicroImaging Inc. Stemi SV11 M²BIO stereo dissecting microscope (Kramer Scientific Corp.) equipped with a DAGE-MTI DC2000 CCD camera. pBoc rhythmicity in individual worms was assessed by calculating coefficient of variance (CV), which is the standard deviation expressed as a percent of the mean.

Dissection and Fluorescence Imaging of Intestines

Calcium oscillations and waves were measured in isolated intestines as described previously (Espelt et al., 2005). In brief, worms were placed in control saline (137 mM NaCl, 5 mM KCl, 1 mM $MgCl_2$, 1 mM $MgSO_4$, 0.5 mM $CaCl_2$, 10 mM HEPES, 5 mM glucose, 2 mM L-asparagine, 0.5 mM L-cysteine, 2 mM L-glutamine, 0.5 mM L-methionine, 1.6 mM L-tyrosine, 28 mM sucrose, pH 7.3, 340 mOsm) and cut behind the pharynx using a 26-gauge needle.

Published September 11, 2006

The hydrostatic pressure in the worm spontaneously extruded the intestine, which remained attached to the rectum and the posterior end of the animal. Isolated intestines were incubated for 15 min in bath saline containing 5 μM fluo-4 AM and 1% BSA. Imaging was performed at room temperature (21–22°C) using a Nikon TE2000 inverted microscope, a Superfluor 40X/1.3 N.A. oil objective lens, a Photometrics Cascade 512B cooled CCD camera (Roper Industries), and MetaFluor software (Universal Imaging Corporation). Fluo-4 was excited using a 490-500BP filter, and a 523-547BP filter was used to detect fluorescence emission. Changes in fluo-4 intensity were quantified using region-of-interest selection and MetaFluor software (Universal Imaging Corporation).

Calcium oscillation period, rise time (RT), and fall time (FT) were quantified as described previously (Prakash et al., 1997; Espelt et al., 2005). Fluorescence images were typically acquired at 0.2 Hz to avoid photobleaching and damage to the intestinal epithelium. However, when Ca^{2+} wave velocity and Ca^{2+} spike rise and fall times were quantified, images were acquired at 1 Hz.

C. elegans Embryonic Cell Culture and Patch Clamp Electrophysiology

Embryonic cells were cultured on 12-mm-diameter acid-washed glass coverslips using methods described previously (Christensen et al., 2002; Estevez et al., 2003). Intestinal cells were identified in culture by expression of the intestine-specific reporter *elt-2*::GFP (Fukushige et al., 1998; Estevez et al., 2003).

Coverslips with cultured embryo cells were placed in the bottom of a bath chamber (model R-26G; Warner Instrument Corp.) that was mounted onto the stage of a Nikon TE2000 inverted microscope. Cells were visualized by fluorescence and video-enhanced DIC microscopy. Patch electrodes were pulled from soft glass capillary tubes (PG10165-4; World Precision Instruments) that had been silanized with dimethyl-dichloro silane. Pipette resistance was 4–7 MΩ. Bath and pipette solutions contained 145 mM NaCl, 20 mM $CaCl_2$, 10 mM HEPES, 20 mM glucose, pH 7.2 (adjusted with NaOH), 345–350 mOsm, and 147 mM sodium gluconate (NaGluconate), 0.6 mM $CaCl_2$, 6 mM $MgCl_2$, 10 mM BAPTA, 10 mM HEPES, 10 μM IP_3, pH 7.2 (adjusted with CsOH), 330 mOsm, respectively.

Whole-cell currents were recorded using an Axopatch 200B (Axon Instruments) patch clamp amplifier. Command voltage generation, data digitization, and data analysis were performed on a 1.6 GHz Pentium computer (Dimension 4400; Dell Computer Corp.) using a Digidata 1322A AD/DA interface with pClamp 8.2 and Clampfit 8.2 software (Axon Instruments). Electrical connections to the amplifier were made using Ag/AgCl wires and 3 M KCl/agar bridges. Leak current was defined as the current observed immediately after obtaining whole-cell access and was subtracted from all subsequent current records obtained from the cell.

RNA Interference

RNA interference was induced by feeding worms bacteria producing dsRNA (e.g., Kamath et al., 2000; Rual et al., 2004). s*tim-1* and *sca-1* RNAi bacterial strains were obtained from the ORF-RNAi feeding library (Open Biosystems) or from cDNAs generated by PCR. The ORF-RNAi *stim-1* bacterial strain produced dsRNA that targeted the first eight exons of the gene, which encode amino acids 1–390 (see Fig. 1). For cameleon imaging studies, a *stim-1* cDNA was generated by PCR and inserted into the RNAi feeding vector pPD129.36. dsRNA produced from this cDNA targeted amino acids 79–289 of the STIM-1 protein. BLAST searches of *C. elegans* genomic and EST databases failed to identify genes with homology to *stim-1*, indicating that off-target effects of RNAi are unlikely. GFP dsRNA–producing bacteria were engineered as described previously (Yin et al., 2004). Bacterial strains were streaked to single colonies on agar plates containing 50 μg/ml ampicillin and 12.5 μg/ml tetracycline. Single colonies were used to inoculate LB media containing 50 μg/ml ampicillin and cultures were grown at 37°C for 16–18 h with shaking. 300 μl of each bacterial culture was seeded onto 60-mm nematode growth medium agar plates containing 50 μg/ml ampicillin and 1 mM IPTG to induce dsRNA synthesis. After seeding, plates were left at room temperature overnight.

For cell culture studies, a *stim-1* DNA template was generated by PCR from the ORF-RNAi clone using T7 primers. dsRNA was synthesized from the DNA template by T7 polymerase reactions (MEGAscript kit; Ambion, Inc.).

Isolated embryo cells were seeded onto glass coverslips in individual wells of four-well culture plates (Nalge Nunc International). The cells were incubated initially with 100 μl of modified (see Christensen et al., 2002) L-15 cell culture medium (Life Technologies) containing 15 μg/ml *stim-1* dsRNA. After 2 h, the culture medium volume was increased to 300 μl and the final dsRNA concentration diluted to 5 μg/ml. An additional 100 μl of modified L-15 containing 5 μg/ml *stim-1* dsRNA was added on the second and third day of culture. Cells were patched clamped 2–3 d after seeding.

Analysis of the Unfolded Protein Response

Synchronized L1 stage *hsp-4*::GFP worms were transferred to RNAi feeding plates seeded with *stim-1* or *sca-1* dsRNA-producing bacteria or bacteria containing the empty feeding vector pPD129.36 as a control. Worms were maintained at 25°C for 30 h. 24 h after feeding was initiated, a group of control worms was transferred for 6 h to another control feeding plate containing 10 μg/ml tunicamycin. Changes in *hsp-4*::GFP fluorescence were determined using a COPAS Biosort (Union Biometrica).

Construction of Transgenes and Transgenic Worms

A full-length *stim-1* cDNA was cloned from *C. elegans* N2 total RNA by RT-PCR. Primers were designed based on the predicted WormBase sequence of Y55B1BM.1. Aspartate residues at positions 55 and 57 were mutated to alanine (i.e., D55A;D57A) using a Quikchange site-directed mutagenesis kit (Stratagene) and confirmed by DNA sequencing. Translational GFP reporters for wild type and D55A;D57A *stim-1* were generated by insertion into vector pPD95.77. Expression of these reporters was driven by 1.9 kb of promoter sequence upstream of the *stim-1* start codon. This sequence was amplified by PCR from *C. elegans* N2 genomic DNA and linked to the *stim-1* cDNA by a PCR fusion-based method (Hobert, 2002). Transgenic worms were generated by DNA microinjection as described by Mello et al. (1991) using *rol-6* as a transformation marker.

An integrated line of worms expressing STIM-1(D55A;D57A)::GFP was generated by exposing 50 P0 *Pstim-1::STIM-1(D55A;D57A)::GFP;rol-6(su1006)* transgenic L4 animals to a dose of 30,000 μJ/cm^2 of UV light that was generated with a UV cross-linker (Hoefer Scientific Instruments). We clonally isolated 500 F1 roller offspring and then isolated two F2 roller offspring from each F1 worm. A single integrated line was then isolated that segregated 100% GFP and *rol-6* positive animals. This line was outcrossed four times to wild-type animals to generate *KbIs15* (*Pstim-1::STIM-1(D55A;D57A)::GFP*; *rol-6* (*su1006*)). As discussed in Results, STIM-1(D55A;D57A)::GFP worms are sterile. To maintain the line, worms were grown on bacteria producing GFP dsRNA.

The yellow cameleon YC6.1 (Truong et al., 2001) was PCR amplified from pcDNA3.1YC6.1 and cloned into the Acc65I and EcoRI sites of the nematode expression vector pFH6.II (Nehrke and Melvin, 2002) to create pKT2. pKT2nhx-2 was created by cloning 4 kb of the *nhx-2* promoter into NheI and SacII sites of pKT2. *nhx-2* encodes an intestine-specific Na^+/H^+ exchanger (Nehrke and Melvin, 2002).

Published September 11, 2006

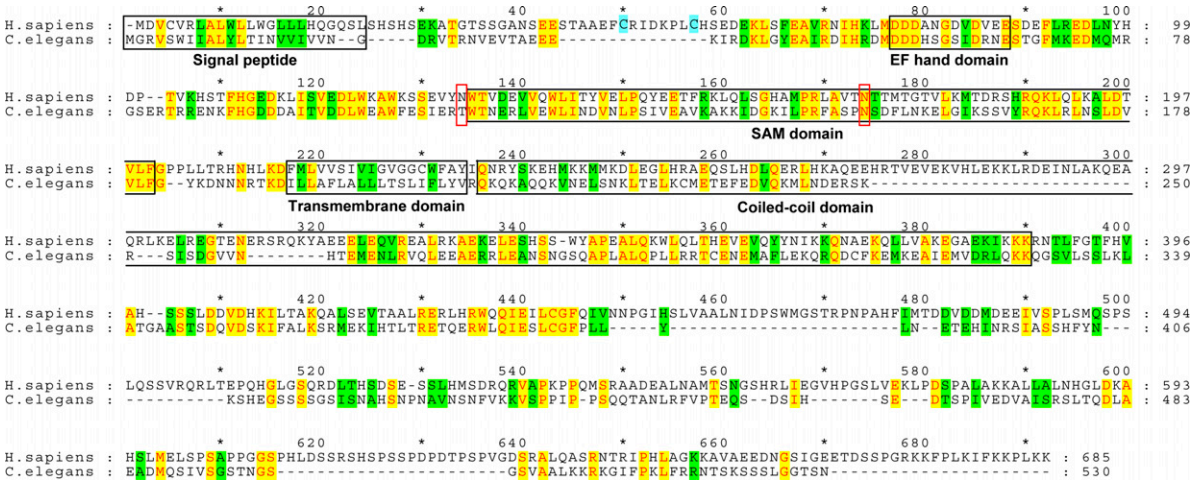

Figure 1. Sequence alignment of human and *C. elegans* STIM1 homologues. Yellow and green shading indicates sequence identity and conserved amino acid substitutions, respectively. Conserved domains are shown in black boxes. Red boxes show location of N-linked glycosylation sites in human STIM1 (Williams et al., 2002). Light blue shading shows N-terminal cysteine residues conserved in human and *Drosophila* STIM homologues. Percent similarity and identity of signal peptide, EF-hand, SAM, transmembrane, and coiled-coil domains are 50.0% and 16.7%, 58.3% and 50.0%, 50.7% and 37.7%, 27.8% and 5.6%, and 57.4% and 21.3%, respectively. Alignment was performed using Vector NTI software (InforMax). Protein domains were identified by SMART (http://smart.embl-heidelberg.de/smart/change_mode.pl).

rde-1(*ne219*) worms were microinjected with a mixture of pKT2nhx-2 and pXXY2004.1rde-1 using *rol-6* as a transformation marker. pXXY2004.1rde-1 encodes wild-type *rde-1* driven by the 4-kb *nhx-2* promoter (Espelt et al., 2005). Roller progeny from these microinjections expressed cameleon YC6.1 and wild-type *rde-1* exclusively in the intestine. Wild-type worms were injected with pKT2nhx-2 and *rol-6* only.

Microscopy

Fluorescence and DIC micrographs were obtained using a Carl Zeiss MicroImaging Inc. M²BIO stereo dissecting microscope and DAGE-MTI DC2000 CCD camera or a Nikon TE2000 inverted microscope and a Micromax CCD-1300 camera (Princeton Instruments). Confocal imaging was performed using an LSM510 confocal microscope equipped with 10×/0.3 N.A. and 40×/1.3 N.A. Plan-Neofluar lenses (Carl Zeiss MicroImaging Inc.). Pixel intensities were quantified using MetaMorph software (Universal Imaging Corporation).

FRET Imaging of Cameleon Protein

Fluorescence resonance energy transfer (FRET) imaging of intestinal cameleon was performed on L3 larvae freely moving on 60-mm agar plates using a Nikon 2000U inverted microscope equipped with a 10× objective lens, monochromatic light source (TILL Photonics), CCD camera detection system (Cooke), and Dual-View beamsplitter (Optical Insights). Cameleon was excited at 435 nm for 100 ms, and 480 nm and 540 nm emissions from the entire intestine were acquired simultaneously at 2 Hz using 2 × 2 binning. The 480/540 nm emission ratio after background subtraction and signal threshholding was used as an indicator of FRET efficiency.

Statistical Analysis

Data are presented as means ± SEM. Statistical significance was determined using Student's two-tailed *t* test for unpaired means. When comparing three or more groups, statistical significance was determined by one-way analysis of variance. P values of ≤0.05 were taken to indicate statistical significance.

RESULTS

A Single STIM Homologue Is Present in the *C. elegans* Genome

BLAST searches of genomic and EST databases demonstrated that a single predicted STIM homologue (gene Y55B1BM.1; GenBank/EMBL/DDBJ accession no. AC024823) is present in the *C. elegans* genome (Williams et al., 2001). We cloned a full-length Y55B1BM.1 cDNA that encoded a 530–amino acid protein with a sequence identical to that of the WormBase-predicted transcript Y55B1BM.1a. The protein encoded by this cDNA has been termed STIM-1 (GenBank/EMBL/DDBJ accession no. DQ812088).

Sequence analysis indicated that STIM-1 is most similar to human STIM1 versus STIM2. Human STIM1 and *Drosophila Stim* possess several conserved domains, including an N-terminal signal peptide, an EF-hand Ca^{2+} binding motif, a SAM domain, a single predicted transmembrane domain, and a large C-terminal region predicted to encode a coiled-coil domain (Williams et al., 2001). These motifs are conserved in *C. elegans* STIM-1 (Fig. 1). The C terminus of human STIM1 contains a serine- and proline-rich domain and a lysine-rich domain. These domains are absent from *Drosophila Stim* (Williams et al., 2001). *C. elegans* STIM-1 also lacks the serine- and proline-rich domain, but a possible lysine-rich domain is present in its C terminus (Fig. 1). Williams et al. (2001) noted that human STIM1 and *Drosophila Stim* contain a pair of cysteine residues that are separated by six amino acids and that are located at similar positions in the N terminus (Fig. 1). These cysteine

Published September 11, 2006

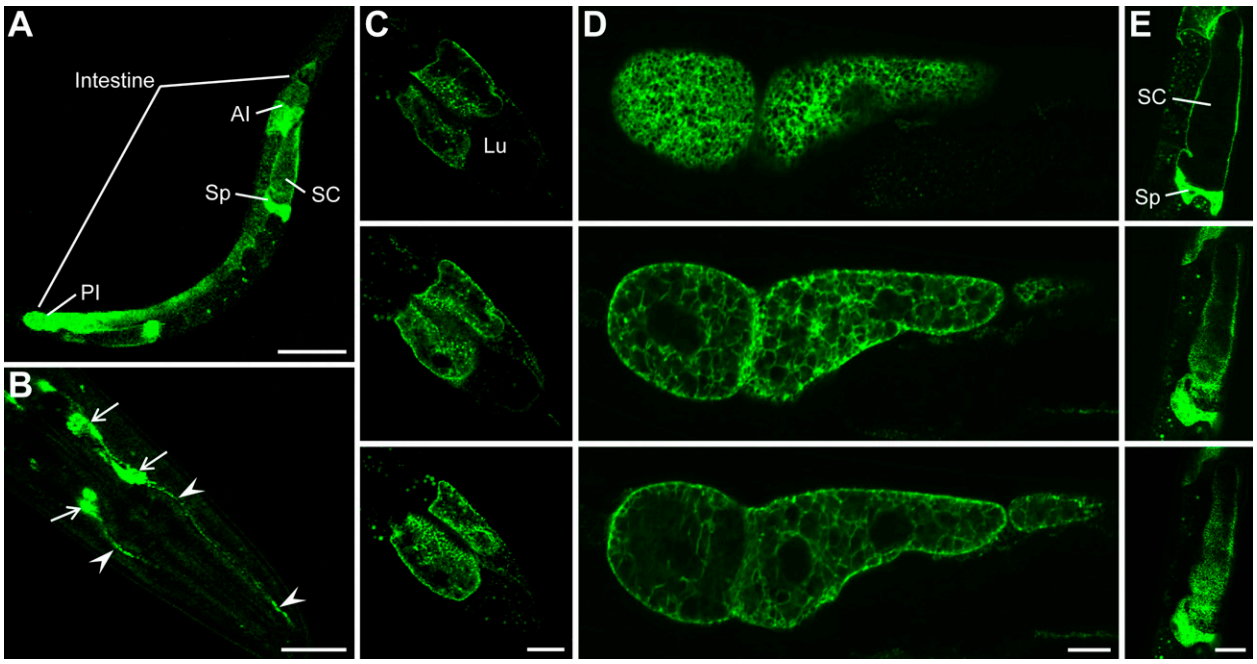

Figure 2. STIM-1::GFP expression pattern. (A) Low magnification confocal image of a whole worm. STIM-1::GFP expression is present throughout the intestine, but is more pronounced in the anterior (AI) and posterior intestine (PI). Expression is also present in the spermatheca (Sp) and gonadal sheath cells (SC). Bar, 100 μm. (B) Expression of STIM-1::GFP in head neurons. Arrows and arrowheads point to cell bodies and dendrites, respectively. Bar, 20 μm. (C) Series of confocal Z-sections through the anterior intestine. STIM-1::GFP appears to be localized to a membrane or submembrane region as well as punctate and presumably intracellular domains. Lu, intestinal lumen. Bar, 20 μm. (D) Series of confocal Z-sections through the posterior intestine. STIM-1::GFP appears to be localized to a membrane and/or submembrane region and a prominent intracellular reticular structure that resembles the intestinal endoplasmic reticulum (Rolls et al., 2002). Bar, 10 μm. (E) Series of confocal Z-sections through the spermatheca (Sp) and gonadal sheath cells (SC). Punctate localization pattern of STIM-1::GFP can be seen in sheath cells in the second and third panels. Bar, 10 μm.

residues are not present in *C. elegans* STIM-1. N-linked glycosylation sites are present in human STIM1 at positions 131 and 171 (Williams et al., 2002; Fig. 1). These sites are conserved in *Drosophila Stim* (Zhang et al., 2005), whereas only the more C-terminal site is present in *C. elegans* STIM-1 (Fig. 1).

STIM-1 Is Expressed in Diverse Cell and Tissue Types

To identify cells in which STIM-1 is expressed, we generated transgenic worms expressing full-length STIM-1 fused to GFP. Expression was driven by 1.9 kb of the *stim-1* promoter located immediately upstream of the start codon. Prominent expression of STIM-1::GFP was detected in the spermatheca, gonad sheath cells, the intestine, and neurons in the head (Fig. 2). Expression was also detected in uterine epithelial cells (unpublished data). STIM-1::GFP-expressing head neurons are likely amphid and/or inner labial (IL) neurons. Inner labial neurons may function in mechanosensation and chemosensation. Amphid neurons function to detect external osmotic, mechanical, and chemical stimuli (Bargmann and Mori, 1997). In vivo Ca^{2+} imaging studies have demonstrated a role for Ca^{2+} signaling in the response of ASH amphid neurons to noxious stimuli (Hilliard et al., 2005).

Expression of STIM-1::GFP in the intestine was heterogeneous. The anterior and posterior intestine expressed the reporter very strongly while expression was weaker in the midsection (Fig. 2 A). Intestinal STIM-1::GFP appeared to be localized to membrane and submembrane regions (Figs. 2, C and D). Confocal Z-sections also revealed a prominent punctate localization in the anterior intestine (Fig. 2 C) and sheath cells (Fig. 2 E). STIM-1::GFP expression showed a striking localization to a reticular structure in the posterior intestine (Fig. 2 D). This reticular structure resembles the ER of *C. elegans* intestinal cells (Rolls et al., 2002). More detailed studies are required to identify the cellular domains in which STIM-1::GFP is expressed.

It should be noted here that the absence of detectable STIM-1::GFP expression in tissues other than those shown in Fig. 2 does not rule out a functional role for STIM-1 in other cell types. The 1.9-kb *stim-1* promoter used in these studies may lack regulatory information required for cell-specific expression. In addition, STIM-1::GFP expression levels may be below detection levels in other tissues. More definitive identification of STIM-1 expression sites awaits the development of suitable antibodies for immunolocalization.

Published September 11, 2006

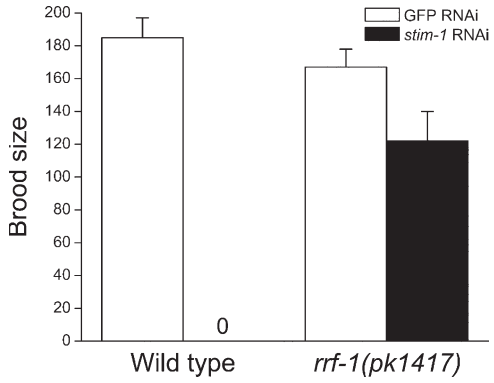

Figure 3. Effect of *stim-1* RNAi on fertility. Brood size is defined as the total number of progeny produced over 4 d. *rrf-1* encodes an RNA-directed RNA polymerase homologue required for RNAi in somatic but not germ cells. *pk1417* is a predicted *rrf-1* null allele (Sijen et al., 2001). Values are means ± SEM (n = 5–8).

STIM-1 Is Required for Fertility and Sheath Cell and Spermatheca Contractile Activity

To begin defining STIM-1 functions, we fed worms STIM-1 dsRNA-expressing bacteria beginning at the L1 larval stage. Young adult *stim-1*(*RNAi*) worms appeared healthy and exhibited no obvious defects in external morphology, movement, or feeding behavior. However, *stim-1*(*RNAi*) worms failed to lay eggs and were completely sterile (Fig. 3).

Somatic cells of *rrf-1*(*pk1417*) mutant worms are resistant to dsRNA, but their germline shows an apparently normal RNAi response (Sijen et al., 2001). To determine whether the sterility phenotype was due to disruption of somatic versus germline cell function, we fed *rrf-1*(*pk1417*) L1 larvae STIM-1 dsRNA-expressing bacteria and analyzed brood size. As shown in Fig. 3, *stim-1* RNAi had no significant ($P > 0.05$) effect on brood size in *rrf-1*(*pk1417*) mutant worms. This indicates that the sterility induced by STIM-1 dsRNA is due largely to dysfunction of somatic cells.

Adult *C. elegans* hermaphrodites possess two U-shaped gonad arms connected via spermatheca to a common uterus. Oocytes form in the proximal gonad and accumulate in a single-file row of graded developmental stages. Developing oocytes remain in diakinesis of prophase I until they reach the most proximal position in the gonad arm where they undergo meiotic maturation and are then ovulated into the spermatheca for fertilization (for review see Hubbard and Greenstein, 2000).

Oocytes are surrounded by myoepithelial sheath cells (Hall et al., 1999). Prior to ovulation, sheath cells contract weakly at a basal rate of seven to eight contractions/min (McCarter et al., 1999). Release of the EGF-like protein LIN-3 from the maturing oocyte induces ovulation by increasing the rate and force of sheath cell contractions and by triggering opening of the gonad-spermatheca valve (Iwasaki et al., 1996; McCarter et al., 1999; Yin et al., 2004). The contractile activity of both the sheath cells (Yin et al., 2004) and spermatheca (Clandinin et al., 1998; Bui and Sternberg, 2002; Kariya et al., 2004) is regulated by IP_3 and Ca^{2+} signaling.

To determine whether STIM-1 RNAi disrupted sheath cell and/or spermatheca function, we imaged anesthetized worms by DIC microscopy. The gonads of adult worms that had undergone several ovulation attempts were filled with endomitotic oocytes (e.g., Fig. 4 C) that were often stacked on top of one another, causing grossly distorted gonad morphology. We therefore isolated very young adult worms, which allowed us to image the first or second ovulation attempt in the absence of gonad morphology defects.

Fig. 4 shows sheath cell contractile activity in worms fed GFP dsRNA-producing bacteria as a control. The mean rate of basal sheath cell contraction measured at −5 min was six contractions/min (Fig. 4 A) with a mean displacement of 1.1 μm (Fig. 4 B). During ovulation, sheath contraction increased significantly ($P < 0.0001$) to a peak rate of 15 contractions/min (Fig. 4 A). The force of contractions also increased significantly ($P < 0.0001$), as indicated by an increase in mean displacement to 2.1 μm (Fig. 4 B).

Sheath cell contractility was greatly reduced in *stim-1*(*RNAi*) worms. The mean basal and peak ovulatory rates of sheath contraction were 2.5 contractions/min and 6 contractions/min (Fig. 4 A). Both rates were significantly ($P < 0.0001$) different from those observed in GFP RNAi control worms. During ovulation, the force of the sheath contraction increased slightly, but not significantly ($P > 0.07$); mean basal and ovulatory sheath displacement were 0.9 μm and 1.3 μm, respectively (Fig. 4 B). Taken together, these results indicate that STIM-1 plays an essential role in regulating sheath cell contractile activity. Loss of STIM-1 activity reduces the rate and force of sheath contraction.

We also noted that spermatheca function was defective in *stim-1*(*RNAi*) worms. During ovulation, the gonad-spermatheca valve opens, allowing the contracting sheath cells to pull the spermatheca over the maturing oocyte (Hubbard and Greenstein, 2000). In all 12 young adult *stim-1*(*RNAi*) worms examined, the gonad-spermatheca valve failed to open during ovulation attempts. Maturing oocytes were therefore trapped in the gonad where they underwent endomitosis (Fig. 4 C).

To further examine the role of STIM-1 in gonad function, we mutated aspartate residues at positions 55 and 57 to alanine (i.e., D55A and D57A). These residues are located in the predicted Ca^{2+} binding EF-hand domain (Fig. 1). Mutation of the analogous amino acids in *Drosophila* and human STIM1 homologues constitutively activates SOCE (Liou et al., 2005; Zhang et al., 2005) and I_{CRAC} (Spassova et al., 2006). STIM-1(D55A;D57A) was fused to GFP and expression was driven by 1.9 kb of the *stim-1* promoter.

Worms expressing STIM-1::GFP exhibited normal fertility (Fig. 5 A). However, STIM-1(D55A;D57A)::GFP

Published September 11, 2006

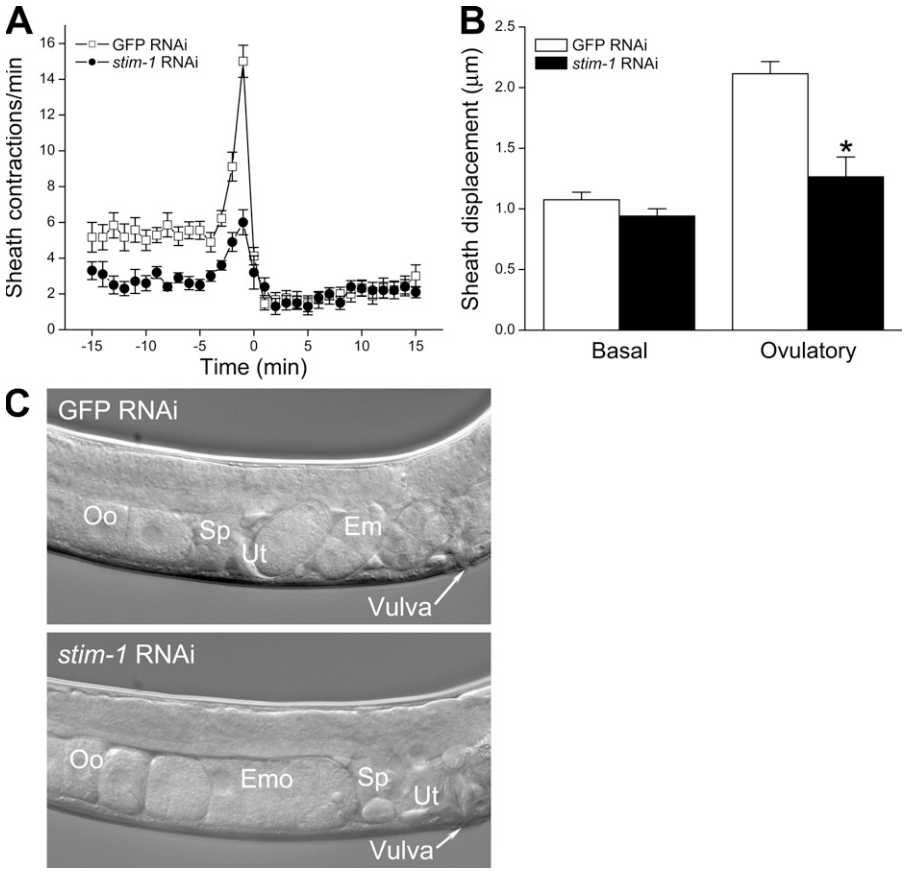

Figure 4. Sheath cell and spermatheca function in control (GFP RNAi) and *stim-1*(*RNAi*) worms. (A) Rates of sheath contraction during a single ovulatory cycle. Time 0 is defined as the time at which ovulation was completed in control worms. *stim-1*(*RNAi*) worms never ovulated (see Results). Therefore in these animals, time 0 is defined as the first time point after peak sheath contraction rate was observed. Values are means ± SEM (n = 9–10). (B) Sheath cell displacement under basal conditions and during ovulation. Basal and ovulatory displacement were measured between −15 and −5 min and between −2 and 0 min, respectively. Values are means ± SEM (n = 6–9). *, $P < 0.0001$ compared with control ovulatory displacement. (C) Differential interference contrast micrographs of control and *stim-1* RNAi worms. Spermatheca fails to open during ovulation in *stim-1*(*RNAi*) worms and oocytes are trapped in proximal gonad where they undergo endomitosis. Em, embryo; Emo, endomitotic oocytes; Oo, oocytes; Sp, spermatheca; Ut, uterus. Note that the uterus in the *stim-1*(*RNAi*) worm is empty, whereas the uterus in the control animal contains three developing embryos.

animals were sterile. This sterility was suppressed by feeding the worms GFP dsRNA-producing bacteria (Fig. 5 A). We did not detect developing embryos or unfertilized oocytes in the uteri of STIM-1(D55A;D57A)::GFP worms, indicating that the fertility defect is due at least in part to defects in ovulation.

In addition to sterility, STIM-1(D55A;D57A)::GFP worms also exhibited a number of other defects. The worms grew more slowly than wild-type animals and their gonads appeared to be stunted and contained endomitotic oocytes (Fig. 5 B). Fluid accumulation was observed in the pseudocoel (Fig. 5 C), suggesting that the EF-hand mutation disrupts whole animal osmoregulation. Large vacuoles were present in the uterus (Fig. 5 D). Smaller vacuoles were observed next to the pharynx (Fig. 5 E) in a location similar to that of STIM-1::GFP-expressing neurons (Fig. 2 B). The vacuoles may be indicators of cell death (e.g., Xu et al., 2001; Bianchi et al., 2004) induced by constitutive activation of STIM-1 and presumably SOCE, which in turn likely disrupts cellular Ca^{2+} homeostasis.

STIM-1 Regulates SOC Channel Activity in Intestinal Epithelial Cells but Is Not Required for IP_3-dependent Oscillatory Ca^{2+} Signaling

The *C. elegans* digestive tract consists of a pharynx, intestine, and rectum. Food is pumped into the pharynx, ground up, and then moved into the intestine for further digestion and nutrient absorption. The intestine is comprised of 20 epithelial cells with extensive apical microvilli. Intestinal epithelial cells secrete digestive enzymes, absorb nutrients, and store lipids, proteins and carbohydrates (White, 1988; Leung et al., 1999; Ashrafi et al., 2003).

Defecation in *C. elegans* is a highly rhythmic process that occurs once every 45–50 s when nematodes are feeding and is mediated by sequential contraction of the posterior body wall muscles, anterior body wall muscles, and enteric muscles (Iwasaki and Thomas, 1997). Posterior body wall muscle contraction (pBoc) is controlled by IP_3-dependent Ca^{2+} oscillations in intestinal epithelial cells (Dal Santo et al., 1999; Espelt et al., 2005; Teramoto and Iwasaki, 2006).

Oscillatory Ca^{2+} signaling is thought to be critically dependent on SOCE (Parekh and Penner, 1997; Venkatachalam et al., 2002; Parekh and Putney, 2005). We therefore examined the effect of *stim-1* knockdown on the defecation cycle. Surprisingly, *stim-1*(*RNAi*) worms had normal defecation rhythms. Mean pBoc periods in control and *stim-1*(*RNAi*) worms were 51 s and 52 s, respectively, and were not significantly ($P > 0.3$) different (Fig. 6 A). The mean coefficient of variance (CV), which is a measure of pBoc cycle rhythmicity (Espelt et al., 2005), was 4.5% in control worms (Fig. 6 B). The low

Published September 11, 2006

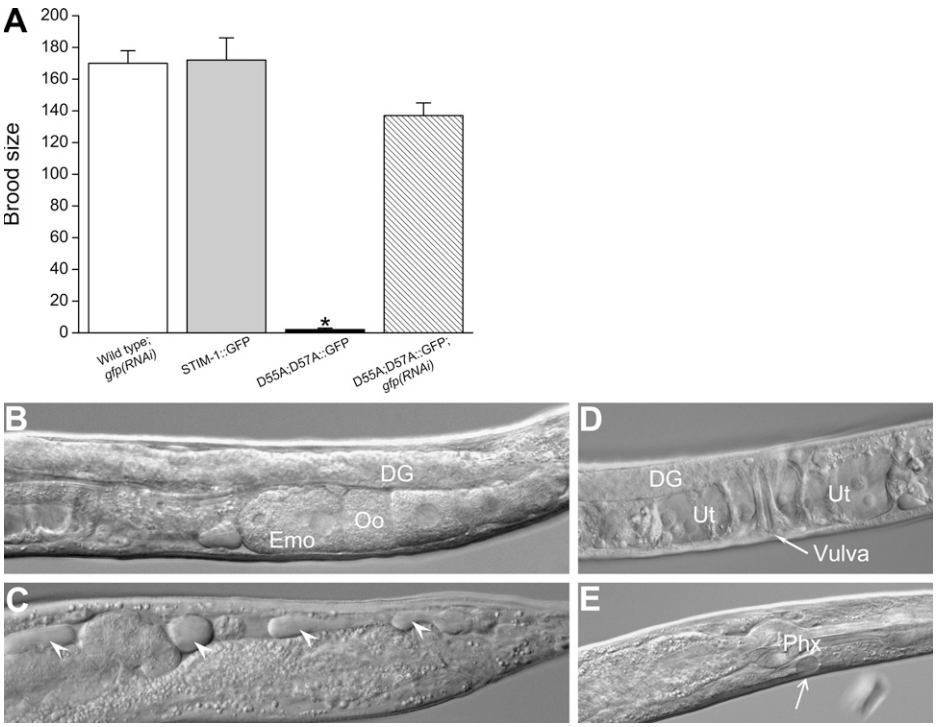

Figure 5. Fertility and morphology defects in transgenic worms expressing the STIM-1 EF-hand mutant D55A;D57A. (A) Brood size in wild type and STIM-1 transgenic worms. Brood size is defined as the total number of progeny produced over 4 d. Wild type;*gfp*(*RNAi*), wild-type worms fed GFP dsRNA–producing bacteria. STIM-1::GFP, transgenic worms expressing STIM-1 GFP fusion protein. D55A;D57A::GFP, transgenic worms expressing STIM-1 EF-hand mutant GFP fusion protein. D55A;D57A::GFP;*gfp*(*RNAi*), transgenic worms expressing STIM-1 EF-hand mutant GFP fusion protein fed GFP dsRNA–producing bacteria. Values are means ± SEM (n = 6–11). *, $P < 0.001$ compared with Wild type;*gfp*(*RNAi*), STIM-1::GFP and D55A;D57A::GFP;*gfp*(*RNAi*) worms. Brood size of D55A;D57A::GFP;*gfp*(*RNAi*) worms was not significantly ($P > 0.05$) different from Wild type:*gfp*(*RNAi*) animals. (B–E) Differential interference contrast micrographs of transgenic worms expressing STIM-1 (D55A;D57A)::GFP. Gonads of STIM-1 (D55A;D57A)::GFP worms appeared to be stunted and contained endomitotic oocytes (B). Fluid accumulation was observed in the pseudocoel (C, arrowheads) and large vacuoles were present in the uterus (D). Smaller vacuoles were observed next to the pharynx (E, arrow) in a location similar to that of STIM-1::GFP-expressing neurons (see Fig. 2 B). DG, distal gonad; Emo, endomitotic oocytes; Oo, oocytes; Phx, pharynx; Ut, uterus.

CV indicates that the pBoc cycle is highly rhythmic. Mean pBoc CV was 5.6% in *stim-1*(*RNAi*) worms and was not significantly ($P > 0.1$) different from that of control animals (Fig. 6 B).

Calcium levels in the ER lumen regulate Ca^{2+} flux through the IP_3R (for review see Burdakov et al., 2005), which in turn modulates the characteristics of intracellular Ca^{2+} oscillations and waves. Mutations in the IP_3R that alter channel activity and regulation could conceivably sensitize IP_3R Ca^{2+} flux to reductions in ER Ca^{2+} levels brought about by a loss of SOCE. We therefore examined the effect of *stim-1* RNAi on worm strains harboring IP_3R mutations.

A single gene, *itr-1*, encodes the IP_3 receptor in *C. elegans* (Baylis et al., 1999; Dal Santo et al., 1999). *sa73* is a loss-of-function *itr-1* allele and *sy290* and *sy327* are gain-of-function alleles. The *sa73* mutation is located in the modulatory region of ITR-1 close to a putative Ca^{2+} binding domain (Dal Santo et al., 1999). *sy290* and *sy327* were isolated as dominant mutations that suppress or "rescue" the phenotype induced by loss-of-function mutations in upstream IP_3 signaling components (Clandinin et al., 1998). *sy290* is an arginine to cysteine substitution at residue 511, which is located in the IP_3 binding domain (Clandinin et al., 1998). This mutation increases in vitro binding affinity for IP_3 approximately twofold (Walker et al., 2002). *sy327* substitutes leucine 899 with phenylalanine in a putative Ca^{2+} binding domain (unpublished data). As shown in Fig. 6, *stim-1* RNAi had no effect on pBoc period or rhythmicity in any of these mutants.

lfe-2 and *ipp-5* encode an IP_3 kinase and phosphatase, respectively (Clandinin et al., 1998; Bui and Sternberg, 2002). Loss-of-function mutations in these genes elevate intracellular IP_3 levels by inhibiting conversion of IP_3 into IP_4 or IP_2 (e.g., Clandinin et al., 1998; Kariya et al., 2004; Espelt et al., 2005). Increased IP_3 levels in turn should increase IP_3R activity and store Ca^{2+} release. In the absence of refilling mechanisms, enhanced Ca^{2+} release may lead to store depletion with subsequent disruption of intracellular Ca^{2+} signals. The effect of *stim-1* RNAi should therefore be enhanced in *lfe-2* and *ipp-5* mutants if SOCE is required for refilling intestinal ER Ca^{2+} stores. However, as shown in Fig. 6, STIM-1 knockdown had no effect on pBoc period or rhythmicity in *lfe-2* and *ipp-5* mutants.

The absence of an effect of *stim-1* RNAi on pBoc in wild type and IP_3 signaling mutants suggests that STIM-1/SOCE does not play a role in generating intestinal Ca^{2+} oscillations. To more directly examine the role of *stim-1* in Ca^{2+} signaling, we used fluo-4 to monitor Ca^{2+} oscillations and waves in isolated intestines. Fig. 7 shows examples of Ca^{2+} oscillations in a control intestine and an intestine isolated from a *stim-1*(*RNAi*) worm.

Published September 11, 2006

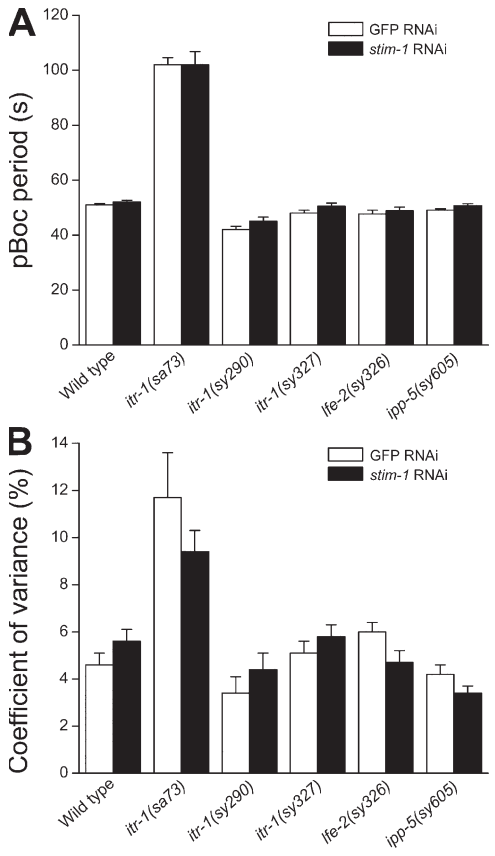

Figure 6. Effect of *stim-1* RNAi on pBoc period (A) and coefficient of variance (B), which is a measure of cycle rhythmicity in wild type and IP_3 signaling mutant worms. *itr-1*(*sa73*) is a loss-of-function allele and *itr-1*(*sy290*) and *itr-1*(*sy327*) are gain-of-function alleles of the *C. elegans* IP_3R. *lfe-2*(*sy326*) and *ipp-5*(*sy605*) are loss-of-function alleles of an IP_3 kinase and IP_3 phosphatase, respectively. Values are means ± SEM (n = 5–19).

The characteristics of intestinal Ca^{2+} oscillations and waves are shown in Table I. *stim-1* RNAi had no significant ($P > 0.1$) effect on oscillation period, oscillation rise and fall time, and Ca^{2+} wave velocity.

As a final test for the role of *stim-1* in intestinal Ca^{2+} signaling, we measured Ca^{2+} oscillations in intact, freely moving worms using the FRET-based Ca^{2+} indicator protein cameleon (Truong et al., 2001). To maximize *stim-1* knockdown, we selectively rescued *rde-1* in the intestines of *rde-1*(*ne219*) loss-of-function mutant worms (see Espelt et al., 2005). *rde-1* (RNAi defective) encodes a protein involved in translation initiation (Tabara et al., 1999; Fagard et al., 2000) and *rde-1* loss-of-function mutants are strongly resistant to RNAi induced by dsRNA injection, feeding, or expression (Tabara et al., 1999). Selective rescue of *rde-1* in the intestine allows normal fertility to be maintained in worms that are fed *stim-1* dsRNA-producing bacteria for multiple successive generations. Fig. 7 (C and D) shows examples of Ca^{2+} oscillations in a worm fed *stim-1* dsRNA-producing bacteria for three generations and a control worm fed bacteria containing empty feeding vector. The mean ± SEM oscillation periods in control and *stim-1*(*RNAi*) worms were 56 ± 4 s (n = 3) and 57 ± 2 s (n = 3), respectively, and were not significantly ($P > 0.8$) different.

The absence of an effect of *stim-1* RNAi on intestinal Ca^{2+} signaling could be due to ineffective knockdown of STIM-1 expression. To address this issue, we examined STIM-1 expression levels in the anterior and posterior intestines of STIM-1::GFP transgenic worms fed *stim-1* dsRNA-producing bacteria. Fig. 8 A shows fluorescence micrographs of the anterior and posterior intestines of wild-type worms, STIM-1::GFP transgenic worms, and transgenic worms fed *stim-1* dsRNA–producing bacteria for 36 h. *stim-1* RNAi dramatically reduced GFP fluorescence in both intestinal regions.

To quantify the effect of *stim-1* RNAi, we measured maximal mean pixel intensity in a 28-μm-wide by 18-μm-high region. *stim-1* RNAi significantly ($P < 0.002$) reduced anterior and posterior intestine pixel intensity by ∼15- and ∼19-fold, respectively (Fig. 8 B). Maximal mean pixel intensity in *stim-1*(*RNAi*) worms was approximately twofold higher than autofluorescence levels detected in wild-type worms. Given that transgenes are typically overexpressed compared with endogenous genes, these results demonstrate that *stim-1* RNAi is highly effective in reducing STIM-1 protein expression.

We also monitored the effect of *stim-1* RNAi on intestinal cell SOC channel activity. Cultured intestinal cells express a SOC channel current with many of the same biophysical characteristics as I_{CRAC} (Estevez et al., 2003). Fig. 9 A shows typical activation of I_{SOC} in a control intestinal cell patch clamped with a pipette solution containing 10 μM IP_3, 10 mM BAPTA, and a free Ca^{2+} concentration of ∼18 nM. Treatment of cultured intestinal cells with *stim-1* dsRNA for 2–3 d eliminated I_{SOC} in 7 of 10 patch-clamped cells (Figs. 9, B and C). Mean ± SEM peak I_{SOC} was reduced nearly 18-fold ($P < 0.02$) from −19.4 ± 6.2 pA/pF (n = 11) in control cells to −1.1 ± 0.7 pA/pF (n = 10) in cells exposed to *stim-1* dsRNA (Fig. 9 C). These results indicate that, as in mammalian and *Drosophila* cells (Liou et al., 2005; Roos et al., 2005; Zhang et al., 2005; Spassova et al., 2006), STIM-1 is a modulator of SOC channels.

Transgenic worms expressing STIM-1(D55A;D57A)::GFP had an increased pBoc cycle time and exhibited striking pBoc arrhythmia (Fig. 10 A, top, and Fig. 10 B). Feeding STIM-1(D55A;D57A)::GFP worms for 52–55 h with bacteria producing *stim-1* dsRNA dramatically suppressed the effect of the EF-hand mutant on pBoc period and rhythmicity (Fig. 10 A, bottom, and Fig. 10 B). Mean pBoc period and CV in STIM-1(D55A;D57A)::GFP;*stim-1*(*RNAi*) animals were 46 s and 7.3%, respectively, and were not significantly ($P > 0.05$) different from wild-type worms (see Fig. 6). Taken together, the electrophysiological, STIM-1::GFP expression, and pBoc data (Figs. 8–10) demonstrate clearly that *stim-1*

Published September 11, 2006

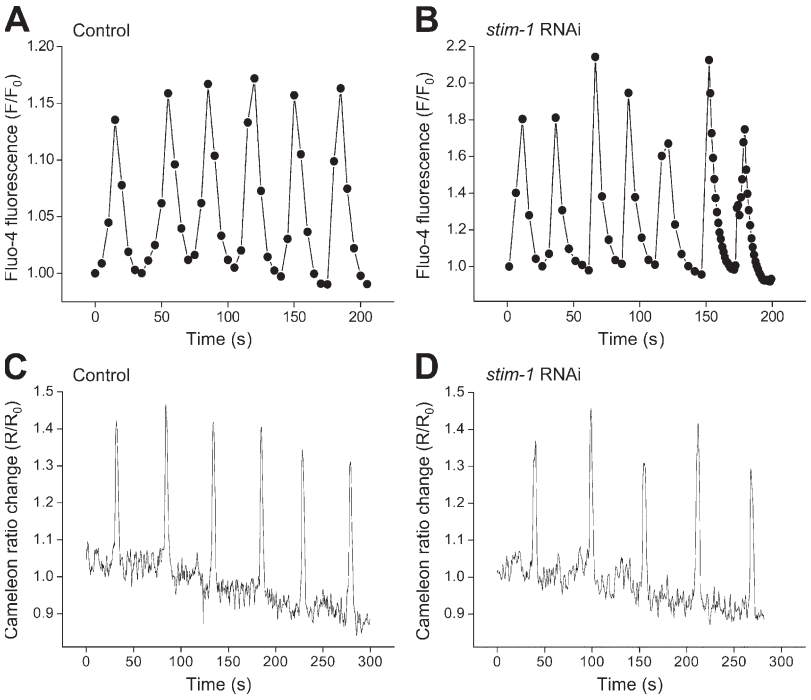

Figure 7. Examples of intestinal Ca^{2+} oscillations. (A and B) Calcium oscillation imaging in dissected intestines loaded with fluo-4. Intestines were isolated from wild-type worms fed either GFP (A) or *stim-1* (B) dsRNA–producing bacteria. Fluorescence images were acquired during the last two oscillations shown in B at 1 Hz. All other images were acquired at 0.2 Hz. (C and D) In vivo Ca^{2+} oscillation imaging in intestines of freely moving L3 larvae expressing the FRET-based Ca^{2+} indicator protein cameleon. Worms were fed bacteria containing the empty RNAi feeding vector (C) or *stim-1* dsRNA–producing bacteria (D) for three successive generations.

RNAi is highly effective in disrupting both STIM-1 expression and SOC activity in the worm intestine.

STIM-1 Is Not Required for Intestinal Cell ER Ca^{2+} Homeostasis under Normal Physiological Conditions

ER Ca^{2+} homeostasis is not only important for intracellular Ca^{2+} signaling, but also for proper protein synthesis and folding. Disruption of ER Ca^{2+} homeostasis triggers the UPR. The UPR is an intracellular signaling and transcriptional/translational program activated by the accumulation of unfolded proteins in the ER lumen (for reviews see Rao et al., 2004; Schroder and Kaufman, 2005). In mammalian cells, inhibition of the sarcoplasmic/ER Ca^{2+} ATPase (SERCA) with thapsigargin depletes ER Ca^{2+} stores and triggers the UPR (e.g., Hong et al., 2004; Durose et al., 2006). We reasoned that if STIM-1 and SOCE were essential for refilling ER Ca^{2+} stores during oscillatory Ca^{2+} signaling, then *stim-1* RNAi should induce the UPR in the worm intestine.

To monitor the intestinal UPR, we used a transgenic worm strain expressing an *hsp-4* transcriptional GFP reporter. *hsp-4* encodes a *C. elegans* homologue of the ER chaperone protein GRP78/BiP and is induced by ER stress (Calfon et al., 2002). As shown in Fig. 11 and as described previously (Calfon et al., 2002), *hsp-4*::GFP is expressed at low levels in the intestine under control conditions. Exposure of worms for 6 h to agar containing 10 μg/ml tunicamycin, which induces ER stress, caused significant ($P < 0.001$) and striking up-regulation of intestinal *hsp-4*::GFP expression (Fig. 11; see also Calfon et al., 2002).

To determine whether store Ca^{2+} depletion activates the UPR in *C. elegans*, we inhibited SERCA by feeding worms *sca-1* dsRNA–producing bacteria for 30 h. *sca-1* encodes the *C. elegans* SERCA homologue (Zwaal et al., 2001). As shown in Fig. 11 B, *sca-1* RNAi caused a nearly threefold increase ($P < 0.001$) in *hsp-4*::GFP expression. However, *hsp-4*::GFP expression was not significantly ($P > 0.05$) altered by *stim-1* RNAi (Fig. 11 B).

In a separate series of experiments, we examined the effect of combined *sca-1* and *stim-1* RNAi on the UPR. As shown in Fig. 11 C, knockdown of both proteins together significantly ($P < 0.0001$) increased whole worm fluorescence ~33% compared with *sca-1* alone.

TABLE I

Effect of stim-1 RNAi on Intestinal Ca^{2+} Oscillations and Waves

Experiment	Oscillation period	Oscillation CV	Oscillation rise time	Oscillation fall time	Wave velocity	No. of waves observed	No. of waves with velocities too rapid to quantify
	s	%	*s*	*s*	*μm/s*		
GFP RNAi	30 ± 3 (6)	18 ± 4 (6)	4 ± 0.1 (6)	10 ± 2 (6)	35 ± 6 (6;15)	22	7
stim-1 RNAi	28 ± 3 (7)	12 ± 3 (7)	5 ± 0.4 (7)	12 ± 1 (7)	24 ± 4 (7;21)	22	1

Values are means ± SEM. Number of observations (*n*) is shown in parentheses. For wave velocity, *n* = number of intestines; number of Ca^{2+} waves.

Published September 11, 2006

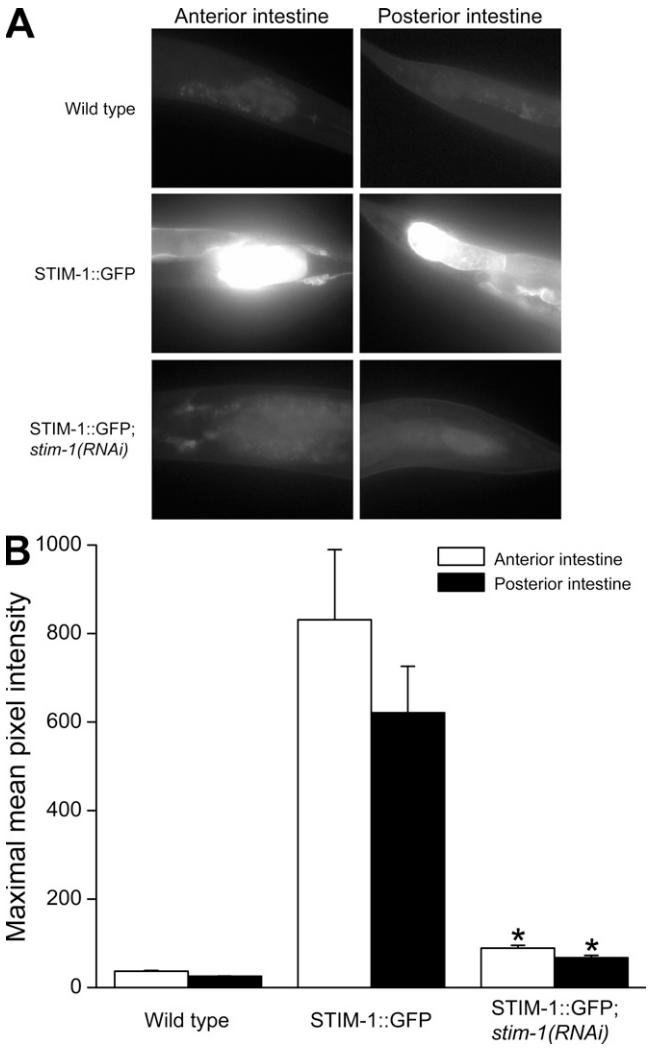

Figure 8. Effect of *stim-1* RNAi on STIM-1::GFP expression. (A) Fluorescence micrographs of anterior and posterior intestines from wild type and STIM-1::GFP worms and STIM-1::GFP worms fed *stim-1* dsRNA–producing bacteria. Images were obtained using a CCD camera and inverted microscope (see Materials and methods). Camera settings were the same for all three groups of worms. Weak fluorescence in wild-type worms is autofluorescence from intestinal granules. (B) Maximal mean pixel intensity in anterior and posterior intestines. Mean pixel intensity was measured in a region 28 μm wide by 18 μm high. The measuring region was positioned over the anterior or posterior intestine at a point where mean pixel intensity was maximal. Values are means ± SEM (n = 7–9). *, $P < 0.002$ compared with STIM-1::GFP worms.

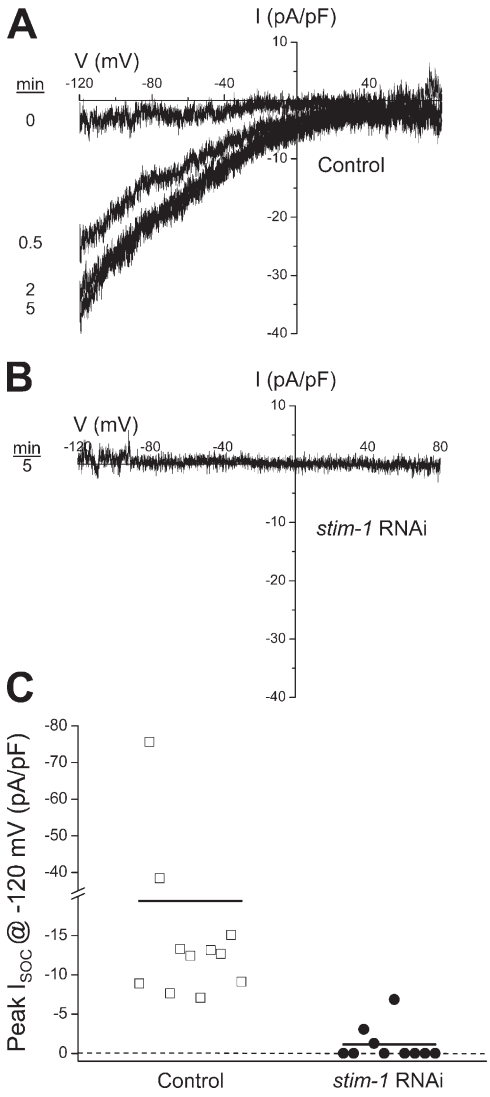

Figure 9. Effect of *stim-1* RNAi on cultured intestinal cell SOC current. Examples of whole cell currents induced by store depletion in a control cell (A) and a cell treated with *stim-1* dsRNA (B). Store depletion was induced using a pipette solution containing 10 μM IP_3, 10 mM BAPTA, and 18 nM free Ca^{2+}. Currents were elicited by ramping membrane voltage from −120 mV to +80 mV at 200 mV/s every 5 s. (C) Effect of *stim-1* dsRNA on peak I_{SOC} measured 5 min after obtaining whole cell access. Solid lines are the mean currents for the cells shown.

Similar results were observed in a second independent experiment (mean ± SEM relative fluorescence values in *sca-1*(*RNAi*) and *sca-1*(*RNAi*);*stim-1*(*RNAi*) worms were 3.2 ± 0.3, n = 21 and 4.2 ± 0.2, n = 121, respectively; $P < 0.008$). Based on the results shown in Figs. 6–11, we conclude that STIM-1 and SOCE do not play significant roles in intestinal cell oscillatory Ca^{2+} signaling or ER Ca^{2+} homeostasis under normal physiological conditions. However, the effects of combined *sca-1* and *stim-1* RNAi on the UPR suggest that SOCE may contribute to the regulation of store Ca^{2+} levels during experimental manipulations that induce extreme store Ca^{2+} depletion.

DISCUSSION

C. elegans STIM-1 overall shares ∼21% amino acid identity with human STIM1 (Fig. 1). The strongest conservation of primary structure occurs in the EF-hand and SAM domains. SAM domains play important roles in mediating protein–protein interactions that regulate the activity, localization, and assembly of numerous

Published September 11, 2006

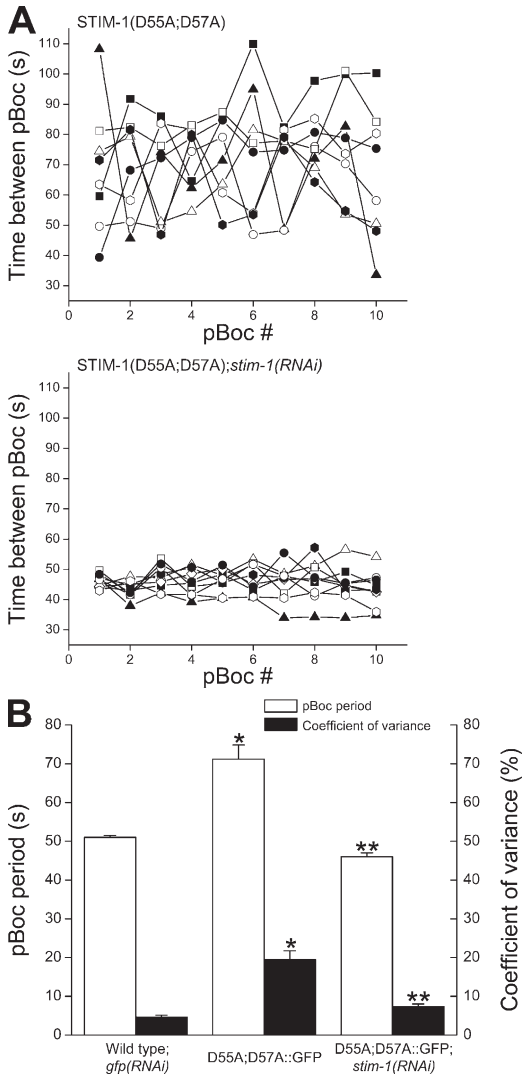

Figure 10. Effect of expression of *stim-1* EF-hand mutation on pBoc period and rhythmicity. (A) pBoc cycles of individual STIM-1 (D55A;D57A)::GFP worms fed bacteria containing the empty vector (top) or fed *stim-1* dsRNA-producing bacteria (bottom). (B) Mean pBoc period and coefficients of variance for wild-type worms and worms shown in A. Wild type;*gfp*(*RNAi*), wild-type worms fed GFP dsRNA–producing bacteria. D55A;D57A::GFP, transgenic worms expressing STIM-1 EF-hand mutant GFP fusion protein fed bacteria containing the empty feeding vector. D55A;D57A::GFP;*stim-1*(*RNAi*), transgenic worms expressing STIM-1 EF-hand mutant GFP fusion protein fed *stim-1* dsRNA–producing bacteria. Values are means ± SEM (n = 8–9). Wild-type data are reproduced from Fig. 6. *, $P < 0.001$ compared with wild-type worms. **, $P < 0.001$ compared with D55A;D57A::GFP worms. pBoc period and coefficient of variance in D55A;D57A::GFP;*stim-1*(*RNAi*) worms were not significantly ($P > 0.05$) different from wild type;*gfp*(*RNAi*) worms.

proteins (Qiao and Bowie, 2005). EF-hands play well-established roles as Ca^{2+} binding sites (Strynadka and James, 1989). Mutagenesis studies indicate that the EF-hand of STIM homologues is likely responsible for monitoring ER lumen Ca^{2+} levels (Liou et al., 2005; Zhang et al., 2005; Spassova et al., 2006). Expression of the STIM-1 EF-hand D55A;D57A mutant under the control of the *stim-1* promoter causes sterility (Fig. 5 A) and pBoc arrhythmia (Fig. 10) as well as morphological abnormalities (Figs. 5, B–E) that are consistent with disruption of Ca^{2+} signaling and possible Ca^{2+}-induced cellular injury.

Interestingly, when we expressed STIM-1(D55A;D57A)::GFP under the control of the promoter for *let-858*, a gene that functions in most *C. elegans* cell types (Kelly et al., 1997), worms showed numerous serious defects and survived very poorly (unpublished data). This suggests that STIM-1 and SOC channels function in more cell types than suggested by GFP reporter studies (Fig. 2) and/or that the EF-hand mutant has cellular effects in addition to SOCE activation. The absence of defects induced by *stim-1* RNAi other than gonad dysfunction does not preclude additional physiological roles for the gene. For example, *stim-1* RNAi–induced sterility (Fig. 3) could obscure a role for STIM-1 in embryonic development. A role for *stim-1* in the *C. elegans* nervous system may have gone undetected in our studies given the relative insensitivity of neurons to RNAi (Simmer et al., 2002). Finally, *stim-1* RNAi could give rise to subtle phenotypes not detected in our assays. It will be valuable in future studies to isolate *stim-1* deletion mutants and perform more extensive physiological and behavioral analyses.

STIM-1 plays an essential role in regulating IP_3-dependent sheath cell and spermatheca contractile activity required for fertility (Figs. 3 and 4). However, despite striking knockdown of STIM-1 expression (Figs. 8 and 10) and intestinal SOC channel activity (Fig. 9), *stim-1* RNAi surprisingly has no effect on oscillatory Ca^{2+} signaling in the intestine (Figs. 6 and 7 and Table I) or on intestinal ER Ca^{2+} homeostasis (Fig. 11). These results can be explained if only a very nominal amount of STIM-1/SOC channel activity, which may remain after RNAi treatment, is required to maintain ER Ca^{2+} levels. Other explanations though are also possible and worth considering. It is widely assumed that SOCE is an essential component of intracellular Ca^{2+} signaling events and is required for maintaining ER Ca^{2+} levels (Parekh and Penner, 1997; Venkatachalam et al., 2002; Parekh and Putney, 2005). With the exception of immune cells (for review see Lewis, 2001), SOCE and CRAC activation in most cell types has not been observed under physiologically relevant conditions, but only under conditions of extreme store depletion experimentally induced by SERCA inhibition, supraphysiological IP_3R activation, exposure to high concentrations of ionomycin, and/or increases in cytoplasmic Ca^{2+} buffering (e.g., Parekh et al., 1997; Golovina et al., 2001; Machaca, 2003). Furthermore, direct demonstration of store Ca^{2+} depletion during intracellular Ca^{2+} oscillations induced by physiologically relevant stimuli is lacking. In the one detailed study conducted to date, little or no change in

Published September 11, 2006

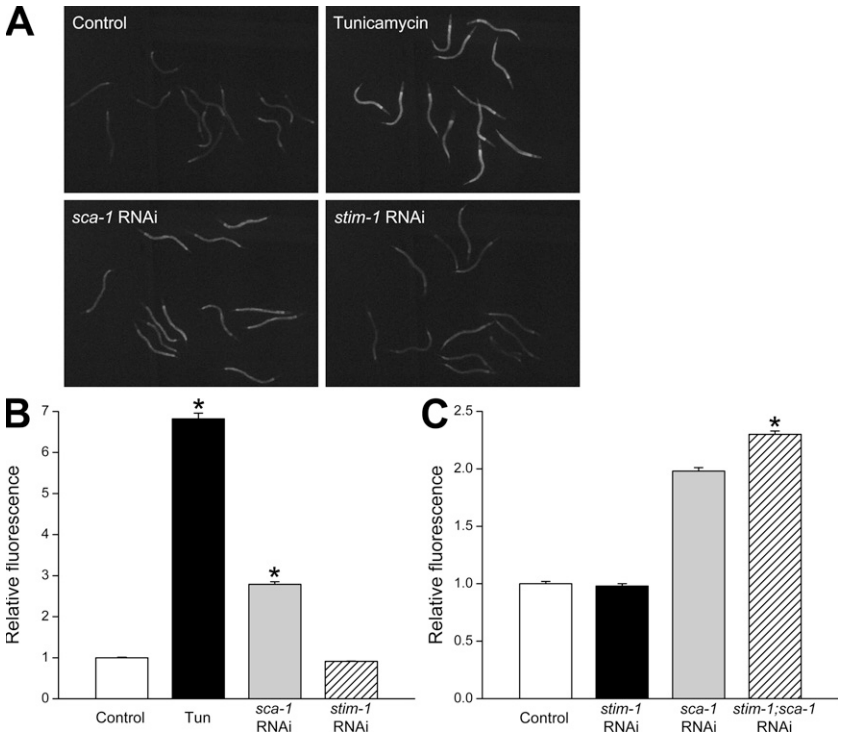

Figure 11. Induction of the intestinal unfolded protein response. (A) Fluorescent micrographs of control *hsp-4*::GFP worms fed bacteria containing the empty feeding vector, control *hsp-4*::GFP worms treated with tunicamycin, and *hsp-4*::GFP worms fed either *sca-1* or *stim-1* dsRNA–producing bacteria. Worms were imaged using a stereo dissecting microscope and CCD camera (see Materials and methods). Images were obtained with identical camera settings. (B) Changes in whole worm fluorescence induced by tunicamycin (Tun), *sca-1* RNAi, or *stim-1* RNAi. Values are means ± SEM (n = 275–732) and are plotted relative to fluorescence in control animals. *, $P < 0.001$ compared with control worms. (C) Effect of combined *sca-1* and *stim-1* RNAi on whole worm fluorescence. Values are means ± SEM (n = 242–756) and are plotted relative to fluorescence in control animals. *, $P < 0.0001$ compared with *sca-1*(*RNAi*) worms. Fluorescence levels in B and C were quantified using a COPAS BioSort and normalized to time-of-flight (i.e., GFP fluorescence/time-of-flight), which is a measure of worm size. Raw GFP fluorescence levels showed an identical pattern of change and statistical significance.

store Ca^{2+} levels was detected during acetylcholine-induced Ca^{2+} oscillations in pancreatic acinar cells. Store depletion was only observed upon supraphysiological acetylcholine stimulation (Park et al., 2000). These results indicate that in acinar cells, SOCE is likely not activated during normal oscillatory Ca^{2+} signaling events. One caveat of these studies is that store depletion may not have been observed if it occurred in ER microdomains that were not resolved by the imaging methods used. However, photobleaching and Ca^{2+} uncaging experiments suggested that the acinar cell ER is a continuous compartment and that Ca^{2+} released from microdomains is rapidly replenished by Ca^{2+} in the bulk ER (Park et al., 2000).

In the worm intestine, it is unclear why SOC channels would be needed to refill stores during oscillatory Ca^{2+} signaling. Patch clamp studies on cultured intestinal cells have demonstrated the presence of a highly Ca^{2+} selective channel, ORCa, that is constitutively active and has biophysical properties resembling those of certain TRPM channels (Estevez et al., 2003; Estevez and Strange, 2005). This channel is likely encoded by the TRPM6/7 homologues *gon-2* and *gtl-1* (Teramoto et al., 2005; unpublished data), both of which are required for maintaining normal intestinal Ca^{2+} oscillations (unpublished data) and pBoc rhythm (Teramoto et al., 2005; unpublished data). Calcium influx through the ORCa channel raises global intracellular Ca^{2+} levels (Estevez and Strange, 2005), and this Ca^{2+} in turn should be available for store refilling. Indeed, in any cell type, non-SOC channel Ca^{2+} entry pathways that are active during Ca^{2+} signaling events could function to refill stores as well as modulate the characteristics of Ca^{2+} signals. A case-in-point is the arachidonic acid–regulated Ca^{2+} channel (ARC) (Mignen and Shuttleworth, 2000). Shuttleworth has argued that ARC is the predominant mode of Ca^{2+} entry during stimulation of certain nonexcitable cell types with physiologically relevant concentrations of agonists and that SOCE is operational only with supraphysiological stimulation (e.g., Shuttleworth, 1999; Shuttleworth and Mignen, 2003).

The widespread existence of SOCE in numerous cell types supports the notion that it must be essential for Ca^{2+} signaling. However, our findings in the *C. elegans* intestine and the arguments outlined above raise the question of whether SOCE is ubiquitously indispensable for the generation and maintenance of Ca^{2+} signals. If it is not indispensable, why are SOC channels expressed in the intestine (Fig. 9; Estevez et al., 2003) and why has SOCE been so widely observed? One possibility is that the primary function of SOCE is to provide cells with a failsafe mechanism for protecting store Ca^{2+} levels during pathophysiological insults and stress conditions. For example, certain viral proteins (Tian et al., 1995; van Kuppeveld et al., 1997) and bacterial toxins (Bryant et al., 2003; Saha et al., 2005) as well as cellular stressors including ischemia (Lehotsky et al., 2003) and oxidants (Henschke and Elliott, 1995; Pariente et al., 2001) induce store Ca^{2+} loss and depletion. Failure to maintain store Ca^{2+} levels under pathophysiological

Published September 11, 2006

and stress conditions can exacerbate injury by disrupting ER protein synthesis and processing and lead ultimately to cell death (Rao et al., 2004; Schroder and Kaufman, 2005). Consistent with this idea, we observed that *stim-1* RNAi had no effect on the intestinal UPR under normal physiological conditions (Fig. 11). However, knockdown of STIM-1 expression enhanced the UPR in worms where Ca^{2+} stores were depleted by *sca-1* (i.e., SERCA) RNAi (Fig. 11 C and Results).

Recent identification of the gene Orai1 (Feske et al., 2006; see also Vig et al., 2006; Zhang et al., 2006) supports the hypothesis that SOCE may not be an essential component of all Ca^{2+} signaling events. Severe combined immunodeficiency (SCID) is a disease caused by defects in immune cell function (Huang and Manton, 2005). A subset of SCID patients has been shown to have defective T cell, B cell, and fibroblast SOCE and T cell I_{CRAC} activation (Partiseti et al., 1994; Le Deist et al., 1995; Feske et al., 2001, 2005). As discussed below, SOCE plays an essential role in T cell activation by antigens (Lewis, 2001). In an elegant study, Feske et al. (2006) used linkage analysis and a *Drosophila* S2 cell genome-wide RNAi screen to identify Orai1 as an essential component of the CRAC channel and as the gene mutated in SCID patient immune cells lacking SOCE. Accumulating evidence suggests that Orai1 likely encodes the CRAC channel itself (Mercer et al., 2006; Peinelt et al., 2006; Soboloff et al., 2006b; Zhang et al., 2006).

Interestingly, in the SCID patients studied by Feske et al. (2000), the only nonimmunological defects observed were nonprogressive muscle hypotonia and mild psychomotor and mental retardation. This finding is unexpected if SOCE plays a ubiquitous and essential role in Ca^{2+} signaling. It is possible that the human Orai1 homologues, Orai2 and Orai3, function as SOC channels in cell types other than T cells, B cells, and fibroblasts. However, only a single Orai homologue is present in the *C. elegans* genome. Our ongoing studies have demonstrated that RNAi knockdown of this gene has no effect on pBoc rhythm but phenocopies the sterility defect and sheath cell and spermatheca dysfunction seen with *stim-1* RNAi (Figs. 3 and 4) (unpublished data). Sterility induced by knockdown of the *C. elegans* Orai1 homologue has also been observed in genome-wide RNAi screens (Maeda et al., 2001; Rual et al., 2004).

While it is unclear whether SOCE plays an essential role in all Ca^{2+} signaling pathways, it is certainly critical for some physiological processes. A role for SOCE in immune cell activation is well established (for review see Lewis, 2001). Stimulation of antigen receptors with antigenic peptides triggers cell replication and a gene transcription program required for the immune response. Antigens induce intracellular Ca^{2+} oscillations that are strictly dependent on extracellular Ca^{2+} influx via CRAC. Evidence suggests that CRAC does more than simply refill stores and may function directly in the generation of Ca^{2+} oscillations (Dolmetsch and Lewis, 1994). The characteristics of Ca^{2+} oscillations in turn increase the efficiency and specificity of gene expression and enhance the detection of low levels of antigens (Dolmetsch et al., 1997, 1998).

In *C. elegans*, STIM-1 and presumably SOCE are essential for regulating the contractile activity of gonad sheath cells and the spermatheca (Fig. 4). The precise functions of SOC channels in these tissues are uncertain. However, it is well established that IP_3 signaling regulates their contractile activity (Clandinin et al., 1998; Bui and Sternberg, 2002; Kariya et al., 2004; Yin et al., 2004). Sheath cell and spermatheca contractile activity may require relatively high and prolonged Ca^{2+} elevation that is dependent on concomitant activation of both store Ca^{2+} release and influx across the plasma membrane. Activation of SOCE in these tissues may be facilitated by limited Ca^{2+} stores that become rapidly depleted during IP_3-regulated Ca^{2+} release. It is also possible that the functional properties of SOC channels are uniquely suited to Ca^{2+} signaling events in the gonad. For example, we have shown previously that a ClC-type anion channel, CLH-3b, is activated in worm oocytes undergoing meiotic maturation and that the channel functions to regulate contraction of surrounding gap junction–coupled sheath cells (Rutledge et al., 2001; Denton et al., 2004). Loss of CLH-3b activity by RNAi (Rutledge et al., 2001) or deletion mutagenesis (unpublished data) causes premature initiation of ovulatory sheath contractions. We have suggested that CLH-3b–induced depolarization of the oocyte and surrounding sheath cells may function to inhibit contraction by inhibiting Ca^{2+} entry through a store-operated CRAC-like channel (Rutledge et al., 2001; Yin et al., 2004). The very high Ca^{2+} selectivity and the lack of voltage-dependent gating of CRAC channels (Lewis, 2001; Parekh and Putney, 2005) facilitate modulation of CRAC-mediated Ca^{2+} influx by membrane voltage changes regulated by other ion channels. This in turn provides mechanisms for increasing the complexity and thus information content of Ca^{2+} signals.

In summary, we have identified a *C. elegans* STIM1 homologue, have demonstrated that it is required for SOC channel activity in intestinal cells, and have shown that it plays essential roles in some but not all IP_3-regulated physiological processes. The exact role of SOCE and SOC channels in the maintenance of store Ca^{2+} levels and in the regulation of Ca^{2+} signaling events in most cell types, with the notable exception of immune cells, is unclear. The breakthrough discoveries of STIM-1 (Roos et al., 2005) and Orai1 (Feske et al., 2006; Vig et al., 2006; Zhang et al., 2006) along with development of appropriate animal and cell models makes it possible to address key questions in the field, including the specific functional roles of SOCE under physiological and pathophysiological conditions and the molecular

mechanisms of SOC channel regulation. Combining powerful forward and reverse genetic analyses with direct physiological measurements of Ca^{2+} signaling and ion channel activity in *C. elegans* should be particularly useful in this regard. A detailed molecular and integrative physiological understanding of SOCE is essential for understanding the role of SOC channels in disease and for the potential development of pharmacological strategies to modulate their activity.

We thank Dr. Joel Rothman (University of California at Santa Barbara, Santa Barbara, CA) for providing the *elt-2*::GFP-expressing worm strain. Other strains used in this work were provided by the *Caenorhabditis* Genetics Center (University of Minnesota, Minneapolis, MN). Confocal microscopy was performed in the Vanderbilt University Medical Center Cell Imaging Shared Resource, which is supported by National Institutes of Health (NIH) grants CA68485, DK20593, DK58404, HD15052, DK59637, and EY08126.

This work was supported by NIH grants GM74229 and DK51610 to K. Strange, and HL08010 to K. Nehrke. T. Lamitina was supported by a postdoctoral fellowship from the National Kidney Foundation.

Olaf S. Andersen served as editor.

Submitted: 27 June 2006
Accepted: 31 August 2006

REFERENCES

Ashrafi, K., F.Y. Chang, J.L. Watts, A.G. Fraser, R.S. Kamath, J. Ahringer, and G. Ruvkun. 2003. Genome-wide RNAi analysis of *Caenorhabditis elegans* fat regulatory genes. *Nature.* 421:268–272.

Bargmann, C.I., and I. Mori. 1997. Chemotaxis and thermotaxis. *In* C. elegans II. D.L. Riddle, T. Blumenthal, B.J. Meyer, and J.R. Priess, editors. Cold Spring Harbor Laboratory Press, Cold Spring Harbor, NY. 717–737.

Barr, M.M. 2003. Super models. *Physiol. Genomics.* 13:15–24.

Baylis, H.A., T. Furuichi, F. Yoshikawa, K. Mikoshiba, and D.B. Sattelle. 1999. Inositol 1,4,5-trisphosphate receptors are strongly expressed in the nervous system, pharynx, intestine, gonad and excretory cell of *Caenorhabditis elegans* and are encoded by a single gene (*itr-1*). *J. Mol. Biol.* 294:467–476.

Berridge, M.J., M.D. Bootman, and H.L. Roderick. 2003. Calcium signalling: dynamics, homeostasis and remodelling. *Nat. Rev. Mol. Cell Biol.* 4:517–529.

Bianchi, L., B. Gerstbrein, C. Frokjaer-Jensen, D.C. Royal, G. Mukherjee, M.A. Royal, J. Xue, W.R. Schafer, and M. Driscoll. 2004. The neurotoxic MEC-4(d) DEG/ENaC sodium channel conducts calcium: implications for necrosis initiation. *Nat. Neurosci.* 7:1337–1344.

Brenner, S. 1974. The genetics of *Caenorhabditis elegans. Genetics.* 77:71–94.

Bryant, A.E., C.R. Bayer, S.M. Hayes-Schroer, and D.L. Stevens. 2003. Activation of platelet gpIIbIIIa by phospholipase C from *Clostridium perfringens* involves store-operated calcium entry. *J. Infect. Dis.* 187:408–417.

Bui, Y.K., and P.W. Sternberg. 2002. *Caenorhabditis elegans* inositol 5-phosphatase homolog negatively regulates inositol 1,4,5-triphosphate signaling in ovulation. *Mol. Biol. Cell.* 13:1641–1651.

Burdakov, D., O.H. Petersen, and A. Verkhratsky. 2005. Intraluminal calcium as a primary regulator of endoplasmic reticulum function. *Cell Calcium.* 38:303–310.

Calfon, M., H. Zeng, F. Urano, J.H. Till, S.R. Hubbard, H.P. Harding, S.G. Clark, and D. Ron. 2002. IRE1 couples endoplasmic reticulum load to secretory capacity by processing the XBP-1 mRNA. *Nature.* 415:92–96.

Christensen, M., A.Y. Estevez, X.M. Yin, R. Fox, R. Morrison, M. McDonnell, C. Gleason, D.M. Miller, and K. Strange. 2002. A primary culture system for functional analysis of *C. elegans* neurons and muscle cells. *Neuron.* 33:503–514.

Clandinin, T.R., J.A. DeModena, and P.W. Sternberg. 1998. Inositol trisphosphate mediates a RAS-independent response to LET-23 receptor tyrosine kinase activation in *C. elegans. Cell.* 92:523–533.

Dal Santo, P., M.A. Logan, A.D. Chisholm, and E.M. Jorgensen. 1999. The inositol trisphosphate receptor regulates a 50-second behavioral rhythm in *C. elegans. Cell.* 98:757–767.

Denton, J., K. Nehrke, E. Rutledge, R. Morrison, and K. Strange. 2004. Alternative splicing of N- and C-termini of a *C. elegans* ClC channel alters gating and sensitivity to external Cl^- and H^+. *J. Physiol.* 555:97–114.

Dolmetsch, R.E., and R.S. Lewis. 1994. Signaling between intracellular Ca^{2+} stores and depletion-activated Ca^{2+} channels generates $[Ca^{2+}]_i$ oscillations in T lymphocytes. *J. Gen. Physiol.* 103:365–388.

D olmetsch, R.E., R.S. Lewis, C.C. Goodnow, and J.I. Healy. 1997. Differential activation of transcription factors induced by Ca^{2+} response amplitude and duration. *Nature.* 386:855–858.

Dolmetsch, R.E., K. Xu, and R.S. Lewis. 1998. Calcium oscillations increase the efficiency and specificity of gene expression. *Nature.* 392:933–936.

Durose, J.B., A.B. Tam, and M. Niwa. 2006. Intrinsic capacities of molecular sensors of the unfolded protein response to sense alternate forms of endoplasmic reticulum stress. *Mol. Biol. Cell.* 17:3095–3107.

Espelt, M.V., A.Y. Estevez, X. Yin, and K. Strange. 2005. Oscillatory Ca^{2+} signaling in the isolated *Caenorhabditis elegans* intestine: role of the inositol-1,4,5-trisphosphate receptor and phospholipases C β and γ. *J. Gen. Physiol.* 126:379–392.

Estevez, A.Y., and K. Strange. 2005. Calcium feedback mechanisms regulate oscillatory activity of a TRP-like Ca^{2+} conductance in *C. elegans* intestinal cells. *J. Physiol.* 567:239–251.

Estevez, A.Y., R.K. Roberts, and K. Strange. 2003. Identification of store-independent and store-operated Ca^{2+} conductances in *Caenorhabditis elegans* intestinal epithelial cells. *J. Gen. Physiol.* 122:207–223.

Fagard, M., S. Boutet, J.B. Morel, C. Bellini, and H. Vaucheret. 2000. AGO1, QDE-2, and RDE-1 are related proteins required for post-transcriptional gene silencing in plants, quelling in fungi, and RNA interference in animals. *Proc. Natl. Acad. Sci. USA.* 97:11650–11654.

Feske, S., R. Draeger, H.H. Peter, K. Eichmann, and A. Rao. 2000. The duration of nuclear residence of NFAT determines the pattern of cytokine expression in human SCID T cells. *J. Immunol.* 165:297–305.

Feske, S., J. Giltnane, R. Dolmetsch, L.M. Staudt, and A. Rao. 2001. Gene regulation mediated by calcium signals in T lymphocytes. *Nat. Immunol.* 2:316–324.

Feske, S., M. Prakriya, A. Rao, and R.S. Lewis. 2005. A severe defect in CRAC Ca^{2+} channel activation and altered K^+ channel gating in T cells from immunodeficient patients. *J. Exp. Med.* 202:651–662.

Feske, S., Y. Gwack, M. Prakriya, S. Srikanth, S.H. Puppel, B. Tanasa, P.G. Hogan, R.S. Lewis, M. Daly, and A. Rao. 2006. A mutation in Orai1 causes immune deficiency by abrogating CRAC channel function. *Nature.* 441:179–185.

Fukushige, T., M.G. Hawkins, and J.D. McGhee. 1998. The GATA-factor *elt-2* is essential for formation of the *Caenorhabditis elegans* intestine. *Dev. Biol.* 198:286–302.

Golovina, V.A., O. Platoshyn, C.L. Bailey, J. Wang, A. Limsuwan, M. Sweeney, L.J. Rubin, and J.X. Yuan. 2001. Upregulated TRP and

enhanced capacitative Ca^{2+} entry in human pulmonary artery myocytes during proliferation. *Am. J. Physiol. Heart Circ. Physiol.* 280:H746–H755.

Hall, D.H., V.P. Winfrey, G. Blaeuer, L.H. Hoffman, T. Furuta, K.L. Rose, O. Hobert, and D. Greenstein. 1999. Ultrastructural features of the adult hermaphrodite gonad of *Caenorhabditis elegans*: relations between the germ line and soma. *Dev. Biol.* 212:101–123.

Henschke, P.N., and S.J. Elliott. 1995. Oxidized glutathione decreases luminal Ca^{2+} content of the endothelial cell ins(1,4,5) P_3-sensitive Ca^{2+} store. *Biochem. J.* 312(Pt 2):485–489.

Hilliard, M.A., A.J. Apicella, R. Kerr, H. Suzuki, P. Bazzicalupo, and W.R. Schafer. 2005. In vivo imaging of *C. elegans* ASH neurons: cellular response and adaptation to chemical repellents. *EMBO J.* 24:63–72.

Hobert, O. 2002. PCR fusion-based approach to create reporter gene constructs for expression analysis in transgenic *C. elegans*. *Biotechniques*. 32:728–730.

Hong, M., M. Li, C. Mao, and A.S. Lee. 2004. Endoplasmic reticulum stress triggers an acute proteasome-dependent degradation of ATF6. *J. Cell. Biochem.* 92:723–732.

Hoth, M., and R. Penner. 1992. Depletion of intracellular calcium stores activates a calcium current in mast cells. *Nature.* 355:353–356.

Huang, H., and K.G. Manton. 2005. Newborn screening for severe combined immunodeficiency (SCID): a review. *Front. Biosci.* 10:1024–1039.

Hubbard, E.J., and D. Greenstein. 2000. The *Caenorhabditis elegans* gonad: a test tube for cell and developmental biology. *Dev. Dyn.* 218:2–22.

Iwasaki, K., J. McCarter, R. Francis, and T. Schedl. 1996. *emo-1*, a *Caenorhabditis elegans* Sec61p gamma homologue, is required for oocyte development and ovulation. *J. Cell Biol.* 134:699–714.

Iwasaki, K., and J.H. Thomas. 1997. Genetics in rhythm. *Trends Genet.* 13:111–115.

Kamath, R.S., M. Martinez-Campos, P. Zipperlen, A.G. Fraser, and J. Ahringer. 2000. Effectiveness of specific RNA-mediated interference through ingested double-stranded RNA in *Caenorhabditis elegans*. *Genome Biol.* 2:RESEARCH0002.

Kariya, K., B.Y. Kim, X. Gao, P.W. Sternberg, and T. Kataoka. 2004. Phospholipase Cε regulates ovulation in *Caenorhabditis elegans*. *Dev. Biol.* 274:201–210.

Kelly, W.G., S. Xu, M.K. Montgomery, and A. Fire. 1997. Distinct requirements for somatic and germline expression of a generally expressed *Caernorhabditis elegans* gene. *Genetics.* 146:227–238.

Le Deist, F., C. Hivroz, M. Partiseti, C. Thomas, H.A. Buc, M. Oleastro, B. Belohradsky, D. Choquet, and A. Fischer. 1995. A primary T-cell immunodeficiency associated with defective transmembrane calcium influx. *Blood.* 85:1053–1062.

Lehotsky, J., P. Kaplan, E. Babusikova, A. Strapkova, and R. Murin. 2003. Molecular pathways of endoplasmic reticulum dysfunctions: possible cause of cell death in the nervous system. *Physiol. Res.* 52:269–274.

Leung, B., G.J. Hermann, and J.R. Priess. 1999. Organogenesis of the *Caenorhabditis elegans* intestine. *Dev. Biol.* 216:114–134.

Lewis, R.S. 2001. Calcium signaling mechanisms in T lymphocytes. *Annu. Rev. Immunol.* 19:497–521.

Liou, J., M.L. Kim, W.D. Heo, J.T. Jones, J.W. Myers, J.E. Ferrell Jr., and T. Meyer. 2005. STIM is a Ca^{2+} sensor essential for Ca^{2+}-store-depletion-triggered Ca^{2+} influx. *Curr. Biol.* 15:1235–1241.

Machaca, K. 2003. Ca^{2+}-calmodulin-dependent protein kinase II potentiates store-operated Ca^{2+} current. *J. Biol. Chem.* 278:33730–33737.

Maeda, I., Y. Kohara, M. Yamamoto, and A. Sugimoto. 2001. Large-scale analysis of gene function in *Caenorhabditis elegans* by high-throughput RNAi. *Curr. Biol.* 11:171–176.

McCarter, J., B. Bartlett, T. Dang, and T. Schedl. 1999. On the control of oocyte meiotic maturation and ovulation in *Caenorhabditis elegans*. *Dev. Biol.* 205:111–128.

Mello, C.C., J.M. Kramer, D. Stinchcomb, and V. Ambros. 1991. Efficient gene transfer in *C. elegans*: extrachromosomal maintenance and integration of transforming sequences. *EMBO J.* 10:3959–3970.

Mercer, J.C., W.I. Dehaven, J.T. Smyth, B. Wedel, R.R. Boyles, G.S. Bird, and J.W. Putney Jr. 2006. Large store-operated calcium-selective currents due to co-expression of Orai1 or Orai2 with the intracellular calcium sensor, Stim1. *J. Biol. Chem.* In press.

Mignen, O., and T.J. Shuttleworth. 2000. $I_{ARC,}$ a novel arachidonate-regulated, noncapacitative Ca^{2+} entry channel. *J. Biol. Chem.* 275:9114–9119.

Miller, M.A., V.Q. Nguyen, M.H. Lee, M. Kosinski, T. Schedl, R.M. Caprioli, and D. Greenstein. 2001. A sperm cytoskeletal protein that signals oocyte meiotic maturation and ovulation. *Science.* 291:2144–2147.

Nehrke, K., and J.E. Melvin. 2002. The NHX family of Na^+-H^+ exchangers in *Caenorhabditis elegans*. *J. Biol. Chem.* 277:29036–29044.

Parekh, A.B., and R. Penner. 1997. Store depletion and calcium influx. *Physiol. Rev.* 77:901–930.

Parekh, A.B., and J.W. Putney Jr. 2005. Store-operated calcium channels. *Physiol. Rev.* 85:757–810.

Parekh, A.B., A. Fleig, and R. Penner. 1997. The store-operated calcium current I_{CRAC}: nonlinear activation by $InsP_3$ and dissociation from calcium release. *Cell.* 89:973–980.

Pariente, J.A., C. Camello, P.J. Camello, and G.M. Salido. 2001. Release of calcium from mitochondrial and nonmitochondrial intracellular stores in mouse pancreatic acinar cells by hydrogen peroxide. *J. Membr. Biol.* 179:27–35.

Park, M.K., O.H. Petersen, and A.V. Tepikin. 2000. The endoplasmic reticulum as one continuous Ca^{2+} pool: visualization of rapid Ca^{2+} movements and equilibration. *EMBO J.* 19:5729–5739.

Parker, N.J., C.G. Begley, P.J. Smith, and R.M. Fox. 1996. Molecular cloning of a novel human gene (D11S4896E) at chromosomal region 11p15.5. *Genomics.* 37:253–256.

Partiseti, M., F. Le Deist, C. Hivroz, A. Fischer, H. Korn, and D. Choquet. 1994. The calcium current activated by T cell receptor and store depletion in human lymphocytes is absent in a primary immunodeficiency. *J. Biol. Chem.* 269:32327–32335.

Peinelt, C., M. Vig, D.L. Koomoa, A. Beck, M.J. Nadler, M. Koblan-Huberson, A. Lis, A. Fleig, R. Penner, and J.P. Kinet. 2006. Amplification of CRAC current by STIM1 and CRACM1 (Orai1). *Nat. Cell. Biol.* 8:771–773.

Prakash, Y.S., M.S. Kannan, and G.C. Sieck. 1997. Regulation of intracellular calcium oscillations in porcine tracheal smooth muscle cells. *Am. J. Physiol.* 272:C966–C975.

Putney, J.W., Jr. 1986. A model for receptor-regulated calcium entry. *Cell Calcium.* 7:1–12.

Qiao, F., and J.U. Bowie. 2005. The many faces of SAM. *Sci. STKE.* 2005:re7.

Rao, R.V., H.M. Ellerby, and D.E. Bredesen. 2004. Coupling endoplasmic reticulum stress to the cell death program. *Cell Death Differ.* 11:372–380.

Rolls, M.M., D.H. Hall, M. Victor, E.H. Stelzer, and T.A. Rapoport. 2002. Targeting of rough endoplasmic reticulum membrane proteins and ribosomes in invertebrate neurons. *Mol. Biol. Cell.* 13:1778–1791.

Roos, J., P.J. DiGregorio, A.V. Yeromin, K. Ohlsen, M. Lioudyno, S. Zhang, O. Safrina, J.A. Kozak, S.L. Wagner, M.D. Cahalan, et al. 2005. STIM1, an essential and conserved component of store-operated Ca^{2+} channel function. *J. Cell Biol.* 169:435–445.

Rual, J.F., J. Ceron, J. Koreth, T. Hao, A.S. Nicot, T. Hirozane-Kishikawa, J. Vandenhaute, S.H. Orkin, D.E. Hill, S. van den Heuvel, and M. Vidal. 2004. Toward improving *Caenorhabditis elegans* phenome mapping with an ORFeome-based RNAi library. *Genome Res.* 14:2162–2168.

Published September 11, 2006

Rutledge, E., L. Bianchi, M. Christensen, C. Boehmer, R. Morrison, A. Broslat, A.M. Beld, A. George, D. Greenstein, and K. Strange. 2001. CLH-3, a ClC-2 anion channel ortholog activated during meiotic maturation in *C. elegans* oocytes. *Curr. Biol.* 11:161–170.

Sabbioni, S., G. Barbanti-Brodano, C.M. Croce, and M. Negrini. 1997. GOK: a gene at 11p15 involved in rhabdomyosarcoma and rhabdoid tumor development. *Cancer Res.* 57:4493–4497.

Saha, S., D.D. Gupta, and M.K. Chakrabarti. 2005. Involvement of phospholipase C in *Yersinia enterocolitica* heat stable enterotoxin (Y-STa) mediated rise in intracellular calcium level in rat intestinal epithelial cells. *Toxicon.* 45:361–367.

Schroder, M., and R.J. Kaufman. 2005. The mammalian unfolded protein response. *Annu. Rev. Biochem.* 74:739–789.

Shuttleworth, T.J. 1999. What drives calcium entry during $[Ca^{2+}]_i$ oscillations?–challenging the capacitative model. *Cell Calcium.* 25:237–246.

Shuttleworth, T.J., and O. Mignen. 2003. Calcium entry and the control of calcium oscillations. *Biochem. Soc. Trans.* 31:916–919.

Sijen, T., J. Fleenor, F. Simmer, K.L. Thijssen, S. Parrish, L. Timmons, R.H. Plasterk, and A. Fire. 2001. On the role of RNA amplification in dsRNA-triggered gene silencing. *Cell.* 107:465–476.

Simmer, F., M. Tijsterman, S. Parrish, S.P. Koushika, M.L. Nonet, A. Fire, J. Ahringer, and R.H. Plasterk. 2002. Loss of the putative RNA-directed RNA polymerase RRF-3 makes *C. elegans* hypersensitive to RNAi. *Curr. Biol.* 12:1317–1319.

Soboloff, J., M.A. Spassova, T. Hewavitharana, L.P. He, W. Xu, L.S. Johnstone, M.A. Dziadek, and D.L. Gill. 2006a. STIM2 is an inhibitor of STIM1-mediated store-operated Ca^{2+} entry. *Curr. Biol.* 16:1465–1470.

Soboloff, J., M.A. Spassova, X.D. Tang, T. Hewavitharana, W. Xu, and D.L. Gill. 2006b. Orai1 and STIM reconstitute store-operated calcium channel function. *J. Biol. Chem.* 281:20661–20665.

Spassova, M.A., J. Soboloff, L.P. He, W. Xu, M.A. Dziadek, and D.L. Gill. 2006. STIM1 has a plasma membrane role in the activation of store-operated Ca^{2+} channels. *Proc. Natl. Acad. Sci. USA.* 103:4040–4045.

Strange, K. 2003. From genes to integrative physiology: ion channel and transporter biology in *Caenorhabditis elegans. Physiol. Rev.* 83:377–415.

Strynadka, N.C., and M.N. James. 1989. Crystal structures of the helix-loop-helix calcium-binding proteins. *Annu. Rev. Biochem.* 58:951–998.

Tabara, H., M. Sarkissian, W.G. Kelly, J. Fleenor, A. Grishok, L. Timmons, A. Fire, and C.C. Mello. 1999. The *rde-1* gene, RNA interference, and transposon silencing in *C. elegans. Cell.* 99: 123–132.

Teramoto, T., and K. Iwasaki. 2006. Intestinal calcium waves coordinate a behavioral motor program in *C. elegans. Cell Calcium.* 40:319–327.

Teramoto, T., E.J. Lambie, and K. Iwasaki. 2005. Differential regulation of TRPM channels governs electrolyte homeostasis in the *C. elegans* intestine. *Cell Metab.* 1:343–354.

Tian, P., M.K. Estes, Y. Hu, J.M. Ball, C.Q. Zeng, and W.P. Schilling. 1995. The rotavirus nonstructural glycoprotein NSP4 mobilizes Ca^{2+} from the endoplasmic reticulum. *J. Virol.* 69:5763–5772.

Truong, K., A. Sawano, H. Mizuno, H. Hama, K.I. Tong, T.K. Mal, A. Miyawaki, and M. Ikura. 2001. FRET-based in vivo Ca^{2+} imaging by a new calmodulin-GFP fusion molecule. *Nat. Struct. Biol.* 8:1069–1073.

van Kuppeveld, F.J., J.G. Hoenderop, R.L. Smeets, P.H. Willems, H.B. Dijkman, J.M. Galama, and W.J. Melchers. 1997. Coxsackievirus protein 2B modifies endoplasmic reticulum membrane and plasma membrane permeability and facilitates virus release. *EMBO J.* 16:3519–3532.

Venkatachalam, K., D.B. van Rossum, R.L. Patterson, H.T. Ma, and D.L. Gill. 2002. The cellular and molecular basis of store-operated calcium entry. *Nat. Cell Biol.* 4:E263–E272.

Vig, M., C. Peinelt, A. Beck, D.L. Koomoa, D. Rabah, M. Koblan-Huberson, S. Kraft, H. Turner, A. Fleig, R. Penner, and J.P. Kinet. 2006. CRACM1 is a plasma membrane protein essential for store-operated Ca^{2+} entry. *Science.* 312:1220–1223.

Walker, D.S., N.J. Gower, S. Ly, G.L. Bradley, and H.A. Baylis. 2002. Regulated disruption of inositol 1,4,5-trisphosphate signaling in *Caenorhabditis elegans* reveals new functions in feeding and embryogenesis. *Mol. Biol. Cell.* 13:1329–1337.

White, J. 1988. The anatomy. *In* The Nematode *Caenorhabditis elegans.* W.B. Wood and the Community of *C. elegans* Researchers, editors. Cold Srping Harbor Press, Cold Spring Harbor, NY. 81–122.

Williams, R.T., S.S. Manji, N.J. Parker, M.S. Hancock, L. Van Stekelenburg, J.P. Eid, P.V. Senior, J.S. Kazenwadel, T. Shandala, R. Saint, et al. 2001. Identification and characterization of the STIM (stromal interaction molecule) gene family: coding for a novel class of transmembrane proteins. *Biochem. J.* 357:673–685.

Williams, R.T., P.V. Senior, L. Van Stekelenburg, J.E. Layton, P.J. Smith, and M.A. Dziadek. 2002. Stromal interaction molecule 1 (STIM1), a transmembrane protein with growth suppressor activity, contains an extracellular SAM domain modified by N-linked glycosylation. *Biochim. Biophys. Acta.* 1596:131–137.

Xu, K., N. Tavernarakis, and M. Driscoll. 2001. Necrotic cell death in *C. elegans* requires the function of calreticulin and regulators of Ca^{2+} release from the endoplasmic reticulum. *Neuron.* 31:957–971.

Yin, X., N.J. Gower, H.A. Baylis, and K. Strange. 2004. Inositol 1,4,5-trisphosphate signaling regulates rhythmic contractile activity of smooth muscle-like sheath cells in the nematode *Caenorhabditis elegans. Mol. Biol. Cell.* 15:3938–3949.

Zhang, S.L., Y. Yu, J. Roos, J.A. Kozak, T.J. Deerinck, M.H. Ellisman, K.A. Stauderman, and M.D. Cahalan. 2005. STIM1 is a Ca^{2+} sensor that activates CRAC channels and migrates from the Ca^{2+} store to the plasma membrane. *Nature.* 437:902–905.

Zhang, S.L., A.V. Yeromin, X.H. Zhang, Y. Yu, O. Safrina, A. Penna, J. Roos, K.A. Stauderman, and M.D. Cahalan. 2006. Genome-wide RNAi screen of Ca^{2+} influx identifies genes that regulate Ca^{2+} release-activated Ca^{2+} channel activity. *Proc. Natl. Acad. Sci. USA.* 103:9357–9362.

Zwaal, R.R., K. Van Baelen, J.T. Groenen, A. van Geel, V. Rottiers, T. Kaletta, L. Dode, L. Raeymaekers, F. Wuytack, and T. Bogaert. 2001. The sarco-endoplasmic reticulum Ca^{2+} ATPase is required for development and muscle function in *Caenorhabditis elegans. J. Biol. Chem.* 276:43557–43563.